

Investigating the Biological Activity of the Novel Hemiketal Eicosanoid E₂

By

Katie Connors Sprinkel

Thesis

Submitted to the Faculty of the
Graduate School of Vanderbilt University
in partial fulfillment of the requirements

for the degree of

MASTER OF SCIENCE

in

Interdisciplinary Studies:
Analytical Pharmacology

May, 2016

Nashville, Tennessee

Approved:

Sean S. Davies, Ph.D.

Claus Schneider, Ph.D.

Brian E. Wadzinski, Ph.D.

TABLE OF CONTENTS

	Page
LIST OF TABLES	v
LIST OF FIGURES	vi
Chapter	
I. Introduction	1
Pathways of enzymatic arachidonic acid oxygenation.....	3
The role of COX-2 and 5-LOX in inflammation: implications for hemiketals.....	5
Co-expression of 5-LOX and COX-2 in inflammatory disease	6
Primary synovial fibroblasts as a model for testing HKE ₂ activity.....	6
Endothelial cells as a model for testing HKE ₂ activity	7
RAW 264.7 cells as a model for testing HKE ₂ activity	7
II. Preparation and Analysis of Synthetic HKE ₂	9
Introduction	9
Results and discussion.....	10
Conclusions	18
III. Testing the Effects of HKE ₂ in Primary Human Synovial Fibroblasts	20
Introduction	20
Results	21
Conclusions	21
IV. Testing the Effects of Hemiketal E ₂ in Human Umbilical Vein Endothelial Cells.....	26
Introduction	26
Results and discussion.....	27
Conclusions	27
V. Testing the Effects of Hemiketal E ₂ in RAW 264.7 Cells	32
Introduction	32
Results and discussion.....	33
Conclusions	37

VI. Materials and Methods	41
Cell lines, cell culture, and reagents	41
HPLC, LC-MS/MS and analytical reagents	41
Tubulogenesis assay	42
WST-1 cell proliferation assay	42
Western blot analysis.....	43
PGE ₂ ELISA.....	44
NFκB reporter assay.....	44
REFERENCES	46

LIST OF TABLES

Table	Page
Table 1. Top hits for 5 μM HKE ₂ from DiscoverX GPCR receptor agonist screen	15
Table 2. Top hits for 5 μM HKE ₂ from DiscoverX GPCR receptor antagonist screen.....	16

LIST OF FIGURES

Figure	Page
Figure 1: Hemiketal eicosanoid biosynthetic pathway	2
Figure 2: Hemiketal eicosanoid E ₂ -methyl ester hydrolysis and purification	11
Figure 3: LC-ESI/MS ² analysis of hemiketal eicosanoid E ₂ (HKE ₂) stability	12
Figure 4: LC-MS/MS analysis of hemiketal eicosanoid E ₂ (HKE ₂) in cell culture medium over time	14
Figure 5: RT-qPCR analysis of hemiketal E ₂ (HKE ₂) modulation of interleukin-1 β induced changes to IL-6 and mPGES-1 gene transcription in primary human synovial fibroblasts.....	23
Figure 6: Western blot analysis of COX-2 expression as modulated by hemiketal eicosanoid E ₂ (HKE ₂) in human primary synovial fibroblasts	24
Figure 7: WST-1 cell proliferation assay to measure the effects of hemiketal eicosanoid E ₂ (HKE ₂) on proliferation of primary human synovial fibroblasts	25
Figure 8: Hemiketal E ₂ (HKE ₂) effects on tubulogenesis in human umbilical vein endothelial cells (HUVECs)	28
Figure 9: Quantification of hemiketal E ₂ (HKE ₂) effects on tubulogenesis in human umbilical vein endothelial cells (HUVECs).....	29
Figure 10: WST-1 cell proliferation assay to measure the effects of hemiketal eicosanoid E ₂ (HKE ₂) on proliferation of human umbilical vein endothelial cells (HUVECs).....	30
Figure 11: Western blot analysis of COX-2 expression as modulated by hemiketal eicosanoid E ₂ (HKE ₂) in RAW 264.7 cells.....	34

Figure 12: ELISA analysis of PGE₂ levels as modulated by hemiketal eicosanoid E₂ (HKE₂) in RAW 264.7 cells35

Figure 13: Effect of hemiketal eicosanoid E₂ (HKE₂) effect on NFκB activation in pNFκB-MetLuc2 stably transfected RAW 264.7 cells36

Figure 14: WST-1 cell proliferation assay to measure the effects of hemiketal eicosanoid E₂ (HKE₂) on proliferation of RAW 264.7 cells38

Figure 15: Fluorescent assay to measure the effects of hemiketal eicosanoid E₂ (HKE₂) on phagocytosis of fluorescently labeled *E. coli* particles39

CHAPTER I

Introduction

Hemiketal eicosanoids (HKs), novel endogenous eicosanoids characterized by Claus Schneider's lab, are produced when 5-lipoxygenase (5-LOX) oxygenates arachidonic acid to form 5*S*-hydroperoxyeicosatetraenoic acid (5*S*-HPETE)^{1,2}. A reduction product of 5*S*-HPETE, 5-hydroxyeicosatetraenoic acid (5*S*-HETE) serves as an efficient substrate for cyclooxygenase-2 (COX-2) (but not cyclooxygenase-1) and leads to the formation of a relatively unstable diendoperoxide (diEP)^{1,2}. COX-2 uses 3 molecules of oxygen to convert 5*S*-HETE to the diEP. The diEP non-enzymatically rearranges to form a mixture of HKs, termed HKE₂ and HKD₂ based on their similarity in structure to prostaglandin E₂ and prostaglandin D₂. HKD₂ also forms enzymatically when the diEP acts as a substrate for hematopoietic prostaglandin D synthase (H-PGDS)^{1,2}. The H-PGDS opens both endoperoxides to form an open chain intermediate that rearranges to HKD₂² (Figure 1). The convergence of 5-LOX and COX-2 pathways suggests a novel mechanism for integrating signaling by both pathways and may have important implications for understanding of inflammation and mechanisms affecting COX-2 inhibition. With HKE₂ now available synthetically, the goal of this project was to begin elucidating the biological activity of HKE₂ in primary synovial fibroblasts, human umbilical vein endothelial cells (HUVECs), and RAW 264.7 cells, each cell type chosen specifically for its relevance to inflammation.

Since HKs are formed in the same physiological context (and by the same biosynthetic enzymes) as prostaglandins (PGs) and leukotrienes (LTs), I hypothesized that the HKE_2 would function in a similar manner: as an autocrine and/or paracrine signaling molecule that mediates

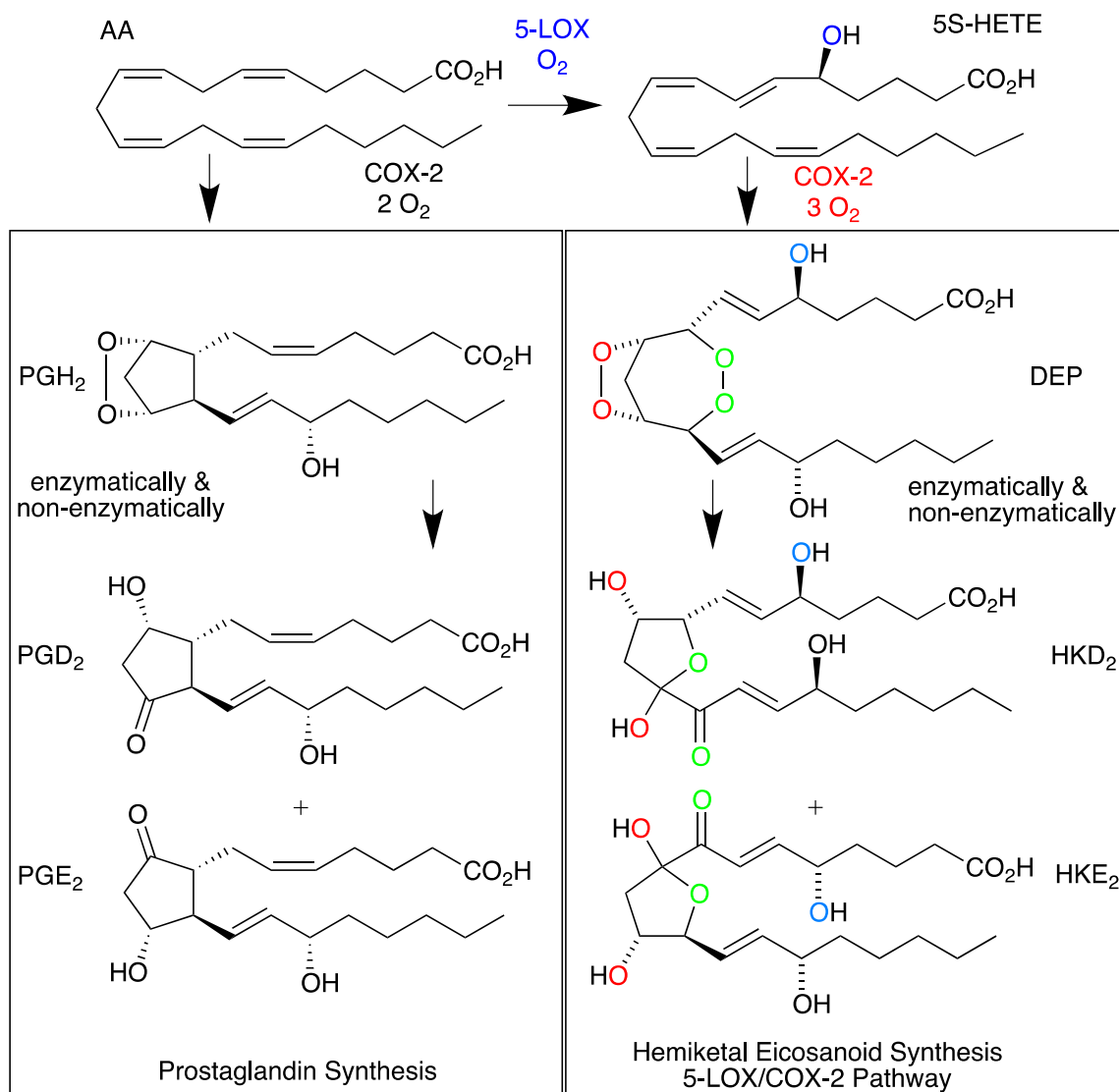


Figure 1: Hemiketal Eicosanoid Biosynthetic Pathway. Hemiketal eicosanoids (HKs) are formed when 5-lipoxygenase (5-LOX) oxygenates arachidonic acid to form 5S-hydroperoxyeicosatetraenoic acid (5S-HPETE)^{1,2}. 5-hydroxyeicosatetraenoic acid (5S-HETE), a reduction product of 5S-HPETE serves as an efficient substrate for cyclooxygenase-2 (COX-2) and leads to the formation of a relatively unstable diendoperoxide (diEP)^{1,2}. COX-2 uses 3 molecules of oxygen to convert 5S-HETE to the diEP, which is non-enzymatically rearranged to form a mixture of HKs, termed HKE_2 and HKD_2 for their similarity in structure to prostaglandin E_2 and prostaglandin D_2 . HKD_2 is also formed enzymatically when the diEP acts as a substrate for H-PGDS^{1,2}. H-PGDS opens both endoperoxides to form an open chain intermediate that rearranges to HKD_2 ^{1,2}

biological activity within the cell of origin, or the nearby environment. I hypothesized that HKE₂ would play a role in the regulation of inflammation and therefore examined its action as a G-protein coupled receptor ligand, in phagocytosis, tubulogenesis, and signaling. HKE₂ is a newly characterized molecule, and as such I have defined some basic parameters relating to its formation and localization.

Pathways of enzymatic arachidonic acid oxygenation

The activity of both 5-LOX and COX-2 are required for the formation of HKs. With the biological function of HKs largely uncharacterized, it is important to discuss the products of 5-LOX and COX-2 individually, as a background for the examination of HK function. Leukotrienes (LTs) and prostaglandins (PGs) play a role in the pathological states such as inflammation, fever, pain, and cancer, as well as in proliferation and angiogenesis³. The oxygenation of arachidonic acid by a LOX or COX enzyme initiates the formation of LTs or PGs, respectively³. Each of the eicosanoid molecules has (or is likely to have) a specific physiological function depending on its environment.

COX oxygenation of arachidonic acid leads to prostaglandins, which are made by most cells within the body. Since prostaglandins are not stored, they must be made *de novo* from arachidonic acid⁴. This is thought to occur at the endoplasmic reticulum and nuclear membrane, where cPLA₂, in response to specific stimuli, frees arachidonic acid from membrane phospholipids⁵. Free arachidonic acid acts as a substrate for cyclooxygenases to form the intermediate prostaglandin PGH₂. From PGH₂, individual synthases form PGE₂, PGD₂, PGF₂, PGI₂, and thromboxane (TxA₂). These prostaglandins mediate inflammatory responses and play a role in vascular homeostasis through their respective G-protein-coupled receptors (GPCRs)³.

The 5-LOX oxygenation of arachidonic acid initiates formation of leukotrienes³. 5-LOX first oxygenates arachidonic acid to 5-HPETE that is then converted in a second LOX reaction to leukotriene A₄ (LTA₄). LTA₄ can be hydrolyzed to leukotriene B₄ (LTB₄) by LTA₄ hydrolase or can be conjugated with reduced glutathione by leukotriene C₄ (LTC₄) synthase. Both LTB₄ and LTC₄ are exported from the cell by specific transporters⁶. The production of leukotrienes occurs in cells such as polymorphonuclear leukocytes, macrophages, and mast cells. 5-LOX is thought to be activated primarily in leukocytes which have migrated into or extravasated through epithelial tissues by pro-inflammatory stimuli⁷. Leukotrienes are critical potentiators of inflammatory responses through their GPCRs and are often associated with bronchoconstriction and asthma^{8,9}.

Aberrant COX and LOX activity is prominently associated with many types of human cancers such as prostate and colorectal cancers, with increased activation of 5-LOX¹⁰. Studies also show that COX-2 activation is associated with early stages of carcinogenesis¹¹. Altered COX and LOX activity has been demonstrated in other inflammatory conditions such as atherosclerosis and Alzheimer's disease (AD). In glioblastoma, the high expression 5-LOX and COX-2 jointly correlate with poor prognosis¹².

The spatial and temporal localization of COX-2 and 5-LOX is highly regulated and is correlated with inflammation. Formation of HKs requires co-localization of active COX-2 and 5-LOX, because the COX-2 substrate (5S-HETE, made by 5-LOX) must be produced in close proximity to active COX-2 enzyme. Instances in which this might occur are when activated neutrophils producing 5S-HETE pass in close proximity to activated endothelial cells or when activated neutrophils producing 5S-HETE are exposed to a vessel wound site where COX-2 expression has increased due to trauma.

The role of COX-2 and 5-LOX in inflammation: implications for hemiketals

A number of studies suggest that the same enzymes are involved in the initiation and resolution of inflammation¹³⁻¹⁵. COX-2 expression during inflammation has been characterized as biphasic¹⁶. The early phase of COX-2 expression was shown experimentally to occur during onset of inflammation, with a second peak coinciding with the resolution phase. PGD₂ synthesis by COX-2 was implicated in the resolution phase, with the non-enzymatic dehydration to the anti-inflammatory J-series of prostaglandins¹⁶. These prostaglandins reduce inflammation by inhibiting the production of cytokines and monocyte activation through activation of PPAR- γ ^{17,18}. Due to the context-dependent action of molecules similar to HKs, investigating the physiological setting in which the HKs are formed may provide insight into their specific function as either pro-inflammatory or pro-resolving lipid mediators.

In addition to leukotrienes, LOX activity also leads to the formation of lipoxins (LXs), which are formed through the subsequent activity of lipoxygenases. LXs act on LX-specific GPCRs to exert their anti-inflammatory activity, as well as act as antagonists of the pro-inflammatory LT receptors^{18,19}. The example of LX formation and function highlights the complex nature of inflammation regulation and provides support for the notion that the convergence of enzymatic pathways may be required for creating products that act as key regulators.

Since both COX-2 and 5-LOX are known to play specific roles in both onset and resolution of inflammation, I hypothesize that the HKs function in same physiological contexts as prostaglandins, leukotrienes, and lipoxins to both drive the onset and establish the resolution of inflammation.

Co-expression of 5-LOX and COX-2 in inflammatory disease

Since our lab has shown that HKs are formed via the convergence of 5-LOX and COX-2 pathways, physiological systems where there is a co-expression of 5-LOX and COX-2 become immediately relevant. In most tissues COX-1 is expressed constitutively and COX-2 is involved in pathological processes. When stimulated, 5-LOX in neutrophils is activated. The 5-LOX expressing-neutrophils may interact with COX-2-expressing macrophages in the blood, or with COX-2 expressing vascular endothelium or in synovial fibroblasts. Neutrophils stimulated for COX-2 expression, then for activation of 5-LOX show the presence of 5S-HETE, LTB₄, PGE₂ and HKE₂ (unpublished data). At sites of vascular inflammation, neutrophils are recruited leading to another instance where cells expressing 5-LOX and COX-2 individually are in immediate proximity. The term “transcellular biosynthesis” can be applied to this type of HK production because neutrophil-derived 5S-HETE crosses to a different cell with activated COX-2 in order to produce HKs. Due to this possible mechanism of HK formation, cell-based experimental models were chosen based on the ability of the specific cell to express COX-2 and the likelihood that the cell would encounter activated 5-LOX expressing neutrophils.

Primary synovial fibroblasts as a model for testing HKE₂ activity

Rheumatoid arthritis is an inflammatory disease of the joints that involves synovial fibroblasts, macrophages, and lymphocytes²⁰. Synovial fibroblasts are cells of the intimal lining layer of synovial tissue. They play a role in the maintenance of joint integrity, but they also act as innate immune cells, attracting neutrophils and producing inflammatory cytokines downstream of Toll-like receptor stimulation²⁰. COX expression in synovial tissue from human patients correlates with mononuclear cell infiltration and RA synovial fibroblasts express more COX than

typical cells²¹. With the ability of synovial fibroblasts to attract 5-LOX expressing neutrophils, synovial fibroblasts from patients with rheumatoid arthritis are an example of where HKs might be made, and thus act.

Endothelial cells as a model For testing HKE₂ activity

At a site of injury within the cardiovascular system, endothelial cells will encounter 5-LOX expressing neutrophils during extravasation and COX-2 expressing macrophages during migration, in a manner similar to synovial fibroblasts encountering activated neutrophils^{22,23}. The proximity of the leukocytes at the endothelium could lead to the production of HKs. Since products of the COX- 2 and 5-LOX pathways have been shown to regulate endothelial cell function and angiogenesis¹¹, the effects of HKD₂ and HKE₂ on tubulogenesis were previously examined in the Schneider lab. Preliminary work showed that HKs stimulated the formation of endothelial capillary-like structures in mouse microvascular pulmonary endothelial cells in a dose-dependent manner (125 nM to 500 nM). The HKs also stimulated endothelial cell migration when used at 1 μM. The same studies show that neither HKD₂ nor HKE₂ (between 10 nM to 1 μM) induced changes in intracellular calcium levels of the endothelial cells nor stimulated their proliferation². For these reasons, primary HUVECs were a relevant model to examine possible effects of HKE₂ activity.

RAW 264.7 cells as a model for testing HKE₂ activity

RAW 264.7 cells are mouse monocyte-like cells that can be stimulated with lipopolysaccharide (LPS) to express COX-2 and become macrophages. These cells can also phagocytosize bacterial particles and engulf 5-LOX expressing neutrophils during

efferocytosis²⁴. Due to their ability to express high levels of COX-2 and their proximity to 5-LOX expressing neutrophils, macrophages are a relevant cell type in which to study the effects of HKE₂.

CHAPTER II

Preparation and Analysis of Synthetic HKE₂

Introduction

Professor Claus Schneider first identified HKE₂ and HKD₂ by incubating synthetic 5S-HETE with recombinant COX-2 in a phosphate buffered-saline (PBS) buffer at pH 8 as part of studies exploring the possible convergence of the 5-LOX and COX-2 pathways. He showed that 5S-HETE, but not 5R-HETE, was a specific and efficient substrate for COX-2, and that oxygenation of 5S-HETE by COX-2 leads to the formation of a chemically unstable bicyclic diEP. This reaction is similar to the oxygenation of AA by COX-2 (which leads to the formation of the chemically unstable intermediate prostaglandin H₂ [PGH₂]) however where COX-2 oxygenation of AA leads to the formation of a cyclopentyl ring, COX-2 oxygenation of 5S-HETE leads to the formation of a seven membered ring due to enzymatic incorporation of one additional molecule of oxygen as compared to PGH₂. Spontaneous nonenzymatic rearrangement of the diEP leads to the formation of HKE₂ and HKD₂ and Prof. Schneider demonstrated that the diEP acts as a substrate for hematopoietic prostaglandin D synthase (H-PGDS), leading to increased formation of HKD₂, over nonenzymatic rearrangement alone². The reaction products were examined and collected using high pressure liquid chromatography (HPLC) with a diode array detector^{1,2}. The structure of the collected products were elucidated using ¹H-NMR. LC-ESI-MS/MS methods were developed using the collected, purified products to characterize retention times and mass spectra. To further study these novel eicosanoids, Prof. Sulikowski synthesized HKE₂-methyl ester (HKE₂-ME). To analyze the product we received from Prof.

Sulikowski, we dissolved the HKE₂-ME film in 100% LC-MS grade methanol and using reverse phase high pressure liquid chromatography with a diode array detector, analyzed and purified the sample. With the final, purified product isolated we also sent HKE₂, dissolved in DMSO, for GPCR screening with DiscoverX against 168 GPCRs and 73 orphan receptors as agonist and antagonist.

Results and discussion

The HKE₂-ME gave a UV maximum absorption of 236 nm and a retention time of 11 min on reversed phase HPLC (Waters Symmetry Shield RP-18 column (2.1 × 100 mm; 3 μm; 1.0 ml/min flow rate over 25 minutes; linear gradient of 80% acetonitrile to 20% acetonitrile in water each containing 10 mM NH₄OAc). Under the same conditions, the free acid hemiketal E₂ (HKE₂) had a retention time of 9.5 min². Since our lab has detected the HKE₂ as a free acid in biological models, we sought to hydrolyze the HKE₂-ME to the HKE₂ for further biological testing. Using 5% KOH, HKE₂-ME was hydrolyzed, subsequently acidified for extraction over solid phase. The hydrolysis product was confirmed to be HKE₂ by LC-ESI-MS and ¹H-NMR. For subsequent routine preparation and purification of the compound, we used UV/Vis-HPLC and monitored the retention time of the compound and the presence of its characteristic absorbance of 236 nm (Figure 2). The yield of HKE₂ from the hydrolysis reaction of the HKE₂-ME with 5% KOH after extraction and purification was approximately 85%. Using the purified HKE₂, verified by ¹H-NMR, we determined the molar extinction coefficient to be 11,000 M⁻¹cm⁻¹. With the HKE₂ purified, we first examined the stability of HKE₂ in RAW 264.7 cell culture medium, Dulbecco's Modified Eagle Medium (DMEM) at 37 °C (similar to cell culture

conditions). We found that HKE₂ levels were not significantly decreased until 4 h following incubation (Figure 3).

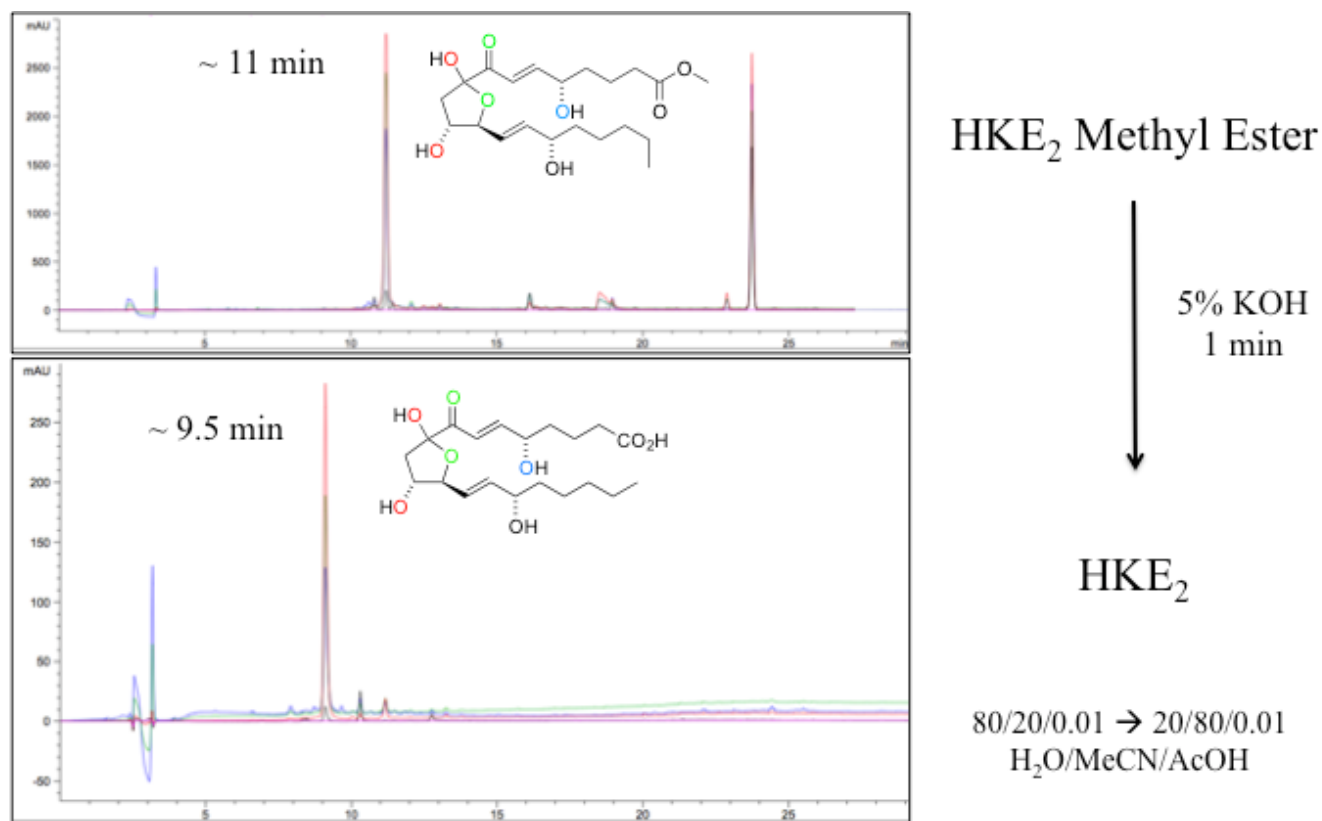


Figure 2: Hemiketal E₂-Methyl Ester (HKE₂-ME) hydrolysis and purification. HKE₂-ME was received from the lab of Professor Gary Sulikowski. The product was hydrolyzed with 5% KOH for 60 s at 23° C. The reaction was neutralized with 1 N HCl, and extracted by solid phase extraction. To analyze the compound before and after cleavage reverse phase high pressure liquid chromatography with a diode array detector was used. The HKE₂-ME, which was verified by ¹H-NMR, has a characteristic retention time of 11 min. After hydrolysis, the hemiketal E₂ (verified by ¹H-NMR) displays a characteristic retention time of 9.5 min. Multiple wavelengths (indicated by different color traces on the HPLC chromatograms) were monitored. HKE₂ displays a characteristic absorbance at 236 nm arising from its conjugated diene moiety and is represented above by an orange trace..

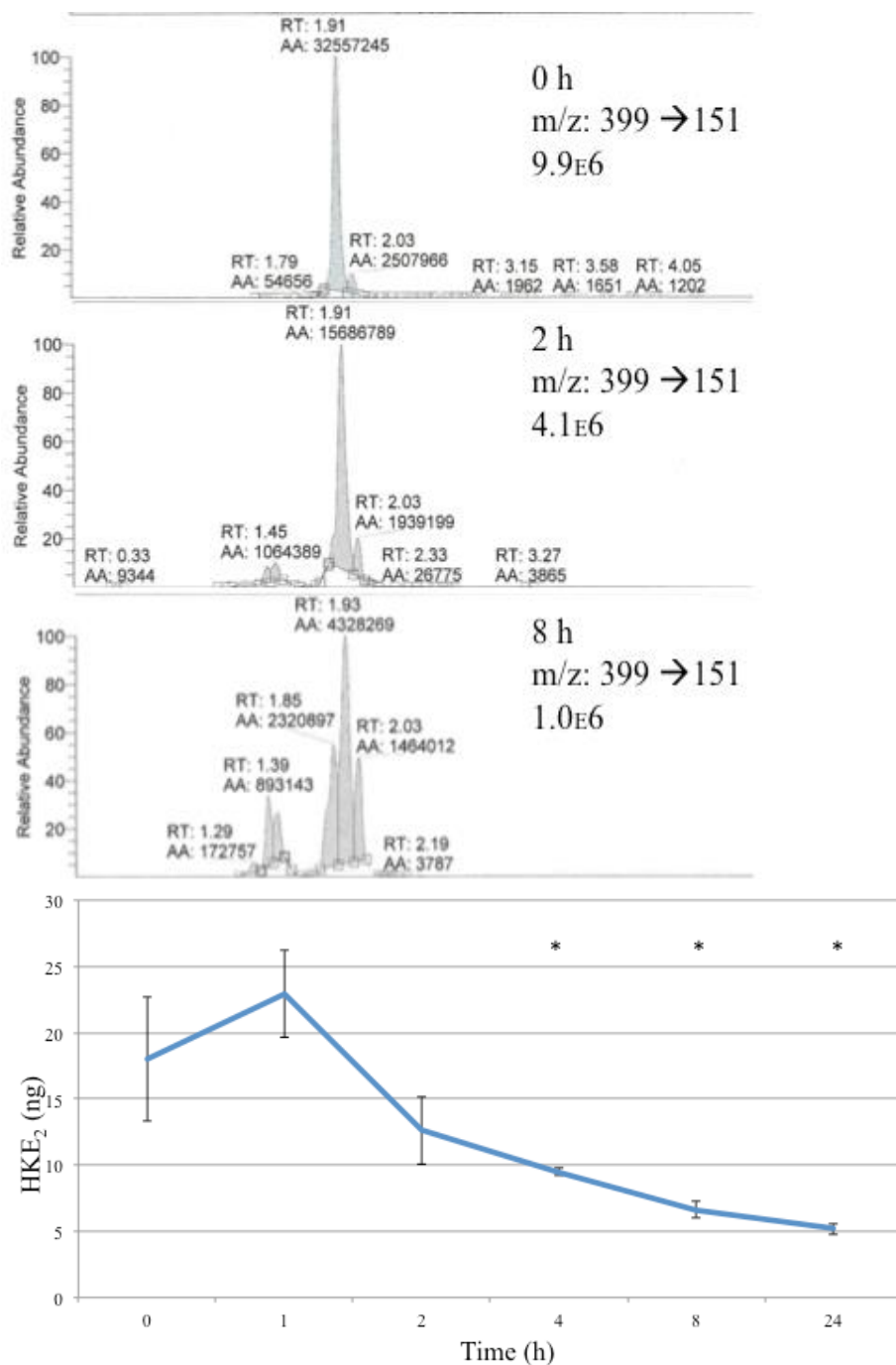


Figure 3: LC-ESI/MS2 analysis of hemiketal E₂ (HKE₂) stability. 25 ng of HKE₂ in methanol (MeOH) was added to 37 °C DMEM and incubated at 37 °C for various lengths of time. The medium was extracted with solid phase extraction cartridges and reactions were quantified against a known quantity of HKE₂. Error bars represent standard error of the mean for the integration of the RT 1.91 peak at various time points. Representative chromatograms are shown above the data (* = p < 0.01, unpaired t test, n = 3).

As HKE₂ is formed by the crossing over of 5-LOX and COX-2, and has been found in the supernatant of human leukocyte preparations, we examined whether exogenously added HKE₂ could be found inside cells. The localization of HKE₂ is relevant to its possible biological activity because a general understanding of localization may provide insight into where HKE₂ might act, for example through cell surface receptors or possibly at other sites within the cell (i.e. through electrophilic adduction). To understand where exogenous HKE₂ localizes, HKE₂ was added to culture medium on RAW 264.7 cells and incubated for various lengths of time at 37 °C. The cell medium was collected and extracted by solid phase. Cells were washed 5 times with 1x PBS, with the last of the 5 washes being collected and extracted by solid phase²⁵. After cells were washed, the aqueous milieu of the cells was extracted by a modified Bligh and Dyer extraction procedure²⁶. The extracts were analyzed by LC-ESI-MS-SRM to determine the presence of HKE₂ inside or outside of the cells. While HKE₂ could not be detected inside the cells (or in the PBS washes) HKE₂ was somehow altered by cells, indicating that HKE₂ may interact in some way with the RAW 264.7 cells, or a factor from the RAW 264.7 cells. We are uncertain as to what factor relating to these cells leads to changes in HKE₂ structure. When HKE₂ is analyzed by LC-ESI-MS/SRM, a characteristic peak at 1.86 min for m/z 399 to 151 is present. In the presence of cells, with increasing time the integration of the peak at 1.86 min decreases, while in a time-dependent manner a peak at 1.35 min appears (also with m/z 399 to 151) (Figure 4). This transformation does not occur in the absence of cells.

The activation of GPCRs would not require that HKE₂ enter the cells, since GPCRs are expressed at the surface of cells. We tested HKE₂ at a maximum concentration of 5 μM as both agonist (Table 1) and antagonist (Table 2). To look at the activation of cell surface receptors

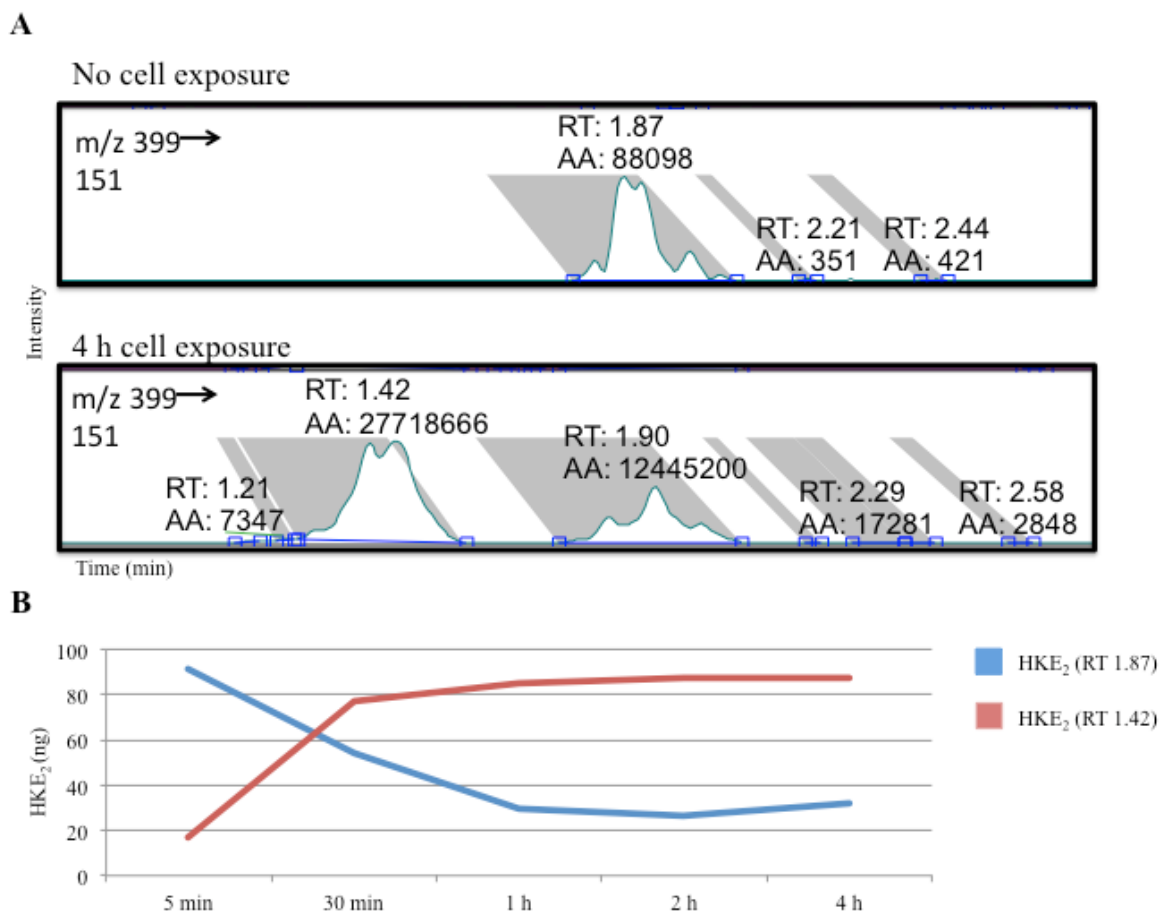


Figure 4. LC-MS/MS analysis of hemiketal eicosanoid E₂ (HKE₂) in cell culture medium over time. (A) A characteristic peak at 1.86 min for m/z 399 to 151 is present (no cells). In the presence of cells, with increasing time the integration of the peak at 1.86 min decreases, while in a time-dependent manner a peak at 1.42 min appears (also with m/z 399 to 151). (B) Integration peaks at 1.87 min and 1.3 min after different lengths of incubation with RAW 264.7 cells (n=2). The lines in (B) are derived from a single experiment and are shown only to visualize the trend of the loss of the peak at 1.86 min and the formation of the peak at 1.42 min.

Table 1	Top Hits for 5 μ M HKE ₂ from DiscoverX GPCR Receptor Agonist Screen					
Target	Baseline	Maximum	HKE ₂	SD	% Activity	CV
CXCR4	963447	2241970	1270240	71163	24	6
HTR1B	617285	1716070	777380	16037	15	2

Table 1: Top hits for 5 μ M hemiketal eicosanoid E₂ (HKE₂) from DiscoverX GPCR Receptor Agonist Screen. CXCR4 or the Chemokine (C-X-C Motif) Receptor 4 showed 24% activity, while the HTR1B or the 5-Hydroxytryptamine Receptor 1B showed 15%.

Table 2 | Top Hits for 5 μ M HKE₂ from DiscoverX GPCR Receptor Antagonist Screen

Target	EC ₈₀	Basal	HKE ₂	SD	% Activity	CV
ADRA2B	650820	197130	545880	39428	23	7
CNR2	858493	372775	720420	1725	28	0
MC1R	65330	14710	50640	4582	29	9
MC3R	300513	125930	255920	10635	26	4
MC5R	223470	72725	178480	14368	30	8
P2RY4	429460	141695	375840	113	19	0
TBXA2R	880280	214495	669080	4412	32	1

Table 2: Top hits for 5 μ M hemiketal eicosanoid E₂ (HKE₂) from DiscoverX GPCR Receptor Antagonist Screen. HKE₂ showed the antagonism of the following receptors at the percentages indicated in the table above: ADRA2B or the Alpha 2B adrenergic receptor, CNR2 or Cannabinoid receptor 2, MC1R, MC3R, MC5R or Melanocortin 1, 3, and 5 receptors (respectively), P2RY4 or Pyrimidinergic receptor P2Y, and TBXA2R or Thromboxane A₂ receptor.

we sent HKE₂ to DiscoverX for screening using proprietary cell-based assays that monitor the activation of a GPCR in a homogenous, non- imaging assay format, using Enzyme Fragment Complementation (EFC) with β - galactosidase (β - Gal) as the functional reporter. The β - Gal enzyme is split into two inactive complementary portions (Enzyme Acceptor [EA] and Enzyme Donor [ED]) and is expressed as fusion proteins in the cell. The EA is fused to β - Arrestin and the ED is fused to the GPCR of interest. When the GPCR is activated and β - Arrestin is recruited to the receptor, ED and EA complementation occurs, restoring β - Gal activity. The β - Gal activity is measured using chemiluminescent detection reagents (PathHunter®). For agonist determination, proprietary cells were incubated with HKE₂ to induce a response. Intermediate dilutions of HKE₂ were made to generate 5X sample in assay buffer. To the cells 5 μ L of 5x sample was added, and the cells were incubated at 37 °C or room temperature for 90 or 180 minutes. For antagonist examination, cells were pre- incubated with HKE₂, followed by agonist challenge at the EC80 concentration. An intermediate dilution of HKE₂ was made to generate 5X sample in assay buffer. As in agonist mode, 5 μ L of 5x sample was added to cells and incubated at 37°C or room temperature for 30 minutes. Then 5 μ L of 6X EC80 agonist in assay buffer was added to the cells and incubated at 37°C or room temperature for 90 or 180 minutes.

The DiscoverX screening revealed that HKE₂ showed activity at several receptors listed in Tables 1 and 2. The agonist table shows the percentage activity of HKE₂ at the relevant receptors. Percent activity was calculated as follows, where RLU is a measure of luminosity: $\% \text{ Activity} = 100\% \times (\text{mean RLU of test sample} - \text{mean RLU of vehicle control}) / (\text{mean MAX control ligand} - \text{mean RLU of vehicle control})$. The table also shows % CV, or the coefficient of variation, which is a measure of relative variability of the data sets. For the receptor hits in agonist mode, it appears that HKE₂ yields 24% activation of CXCR4 (the receptor at which

HKE₂ demonstrated the highest percentage activity), with a 6% coefficient of variation - as compared to 100% activity (set mathematically by the endogenous ligand, in this case CXCL12). While the value of further study of the effect of HKE₂ at CXCR4 cannot be ruled out, this is not a robust hit. To study this further one might consider using cells such as HUVECs, which have been engineered to overexpress CXCR4 and perform dose response curves that examine higher concentrations of HKE₂ than what were used in the DiscoverX screen. Additionally, varying incubation time of HKE₂ may also yield stronger activation of CXCR4 by HKE₂. HKE₂ was also examined as an antagonist, and percentage inhibition was determined as follows: % Inhibition = $100\% \times (1 - (\text{mean RLU of test sample} - \text{mean RLU of vehicle control}) / (\text{mean RLU of EC80 control} - \text{mean RLU of vehicle control}))$. The receptor at which HKE₂ showed the greatest antagonist activity was the Thromboxane Receptor (TBXA₂R). This data reflects that HKE₂ is able to inhibit TBXA₂R 30% (with a % CV of 1). Additional studies, such as monitoring the ability of HKE₂ to inhibit platelet aggregation may be warranted to make more in depth conclusions about HKE₂ as a TXA₂R antagonist. The results from DiscoverX in regards to HKE₂ activity at GPCRs provide an excellent starting point for functional assays testing the effects of HKE₂.

Conclusions

From this work, we conclude that synthetic HKE₂ is structurally identical to the enzymatic HKE₂ based on HPLC, MS/MS, UV-Vis, and NMR. We also determined that HKE₂ may have activity at GPCRs, but the activity of HKE₂ at the receptors tested per DiscoverX screen was modest. We can also conclude that HKE₂ undergoes a chemical change that is dependent on RAW 264.7 cells. This finding suggests the need for a number of subsequent

studies such as those to determine what metabolite(s) form when HKE₂ is transformed by RAW 264.7 cells and the localization of HKE₂ within the cell. Also, because HKE₂ is a highly electrophilic compound that forms inside cells, whether HKE₂ adducts to nucleophilic amino acid residues such as cysteine or serine should be examined.

Chapter III

Testing the Effects of HKE₂ in Primary Human Synovial Fibroblasts

Introduction

Primary human synovial fibroblasts, used in these experiments, are cells isolated from the joints of patients with rheumatoid arthritis (RA), which is a systemic autoimmune inflammatory disease characterized by synovial inflammation, as well as destruction of bone and cartilage^{27,28}. Synovial tissues isolated from patients with inflammatory arthritis produce high levels of PGs, and COX-2 is likely responsible for the increases in PGs^{29,30}. COX-2 is abundant in the endothelial cells of synovial blood vessels³¹, where activated neutrophils would circulate. The synovium in RA produces increased levels of PGE₂. The PGs play critical roles in the dilatation and permeability of small blood vessels²⁹.

Because we wanted models that might reflect environments in which the HKs might be made, we focused on models where both increased 5-LOX and COX-2 expression or activity was important. In addition to increased levels of PGE₂, synovial fibroblasts have been shown to attract neutrophils²⁰, meaning that primary synovial fibroblasts are cells that would come in contact with 5-LOX expressing neutrophils during inflammation, through a mechanism that is, in part, dependent on COX-2 derived products²⁹. Additionally, the lab of Professor Leslie Crofford has shown that microsomal prostaglandin E₂ synthase (mPGES1) is upregulated in primary synovial fibroblasts and is, through a feed forward mechanism, regulated by PGE₂ as well as responsible for PGE₂ production. This suggests that COX-2 derived products regulate inflammation in primary synovial fibroblasts. Because this pathway is not fully elucidated, there appears to be value in investigating whether HKE₂ may act along this feed forward mechanism.

Results

We examined the effects of HKE₂ as it relates to regulation of mPGES1, by measuring RNA transcription of mPGES1 relative to GAPDH. Our results shows that 1 ng/mL IL-1 β stimulation upregulated mPGES1, as would be expected as IL-1 β is an inflammatory stimulus. We also measured the upregulation of IL-6, as a control since IL-6 transcription has been shown to increase downstream of IL-1 β ³². Preincubation with HKE₂ does not significantly alter mPGES1 transcription resulting from IL-1 β stimulation (Figure 5). We also investigated if exogenous HKE₂ treatment would increase levels of COX-2. HKE₂ did not increase levels of COX-2, nor did it potentiate COX-2 expression when pre-incubated with primary human synovial fibroblasts before IL-1 β stimulation (Figure 6). Also, we investigated HKE₂ effect on proliferation of primary synovial fibroblasts using the WST-1 assay. We examined the effects of HKE₂ on fibroblast proliferation because studies have shown that COX-2 activation in fibroblasts may affect proliferation and invasiveness of certain cell types³³. We determined that HKE₂ did not affect proliferation of primary synovial fibroblasts with or without IL-1 β stimulation (Figure 7). Thus, HKE₂ fails to exert any meaningful effect in our models of primary synovial fibroblast activation.

Conclusions

While primary synovial fibroblasts represent a model of inflammation in which HKE₂ might act, we did not detect any effect of HKs in the assays we performed. This limited set of assays does not mean that HKs are not biological active, as there are a number of other activities where lipid mediators may be important. [Please elaborate on one or more of these.] Determining the effects of unknown endogenous compound is, to some extent, like finding a needle in a haystack. Occam's razor would suggest cells able to produce these paracrine or

autocrine signaling molecules are the first that should be examined. In addition to examining the effect of HKE₂ on cell types associated with inflammation, a continued examination of these cell types ability or produce HKE₂ would be interesting to pursue.

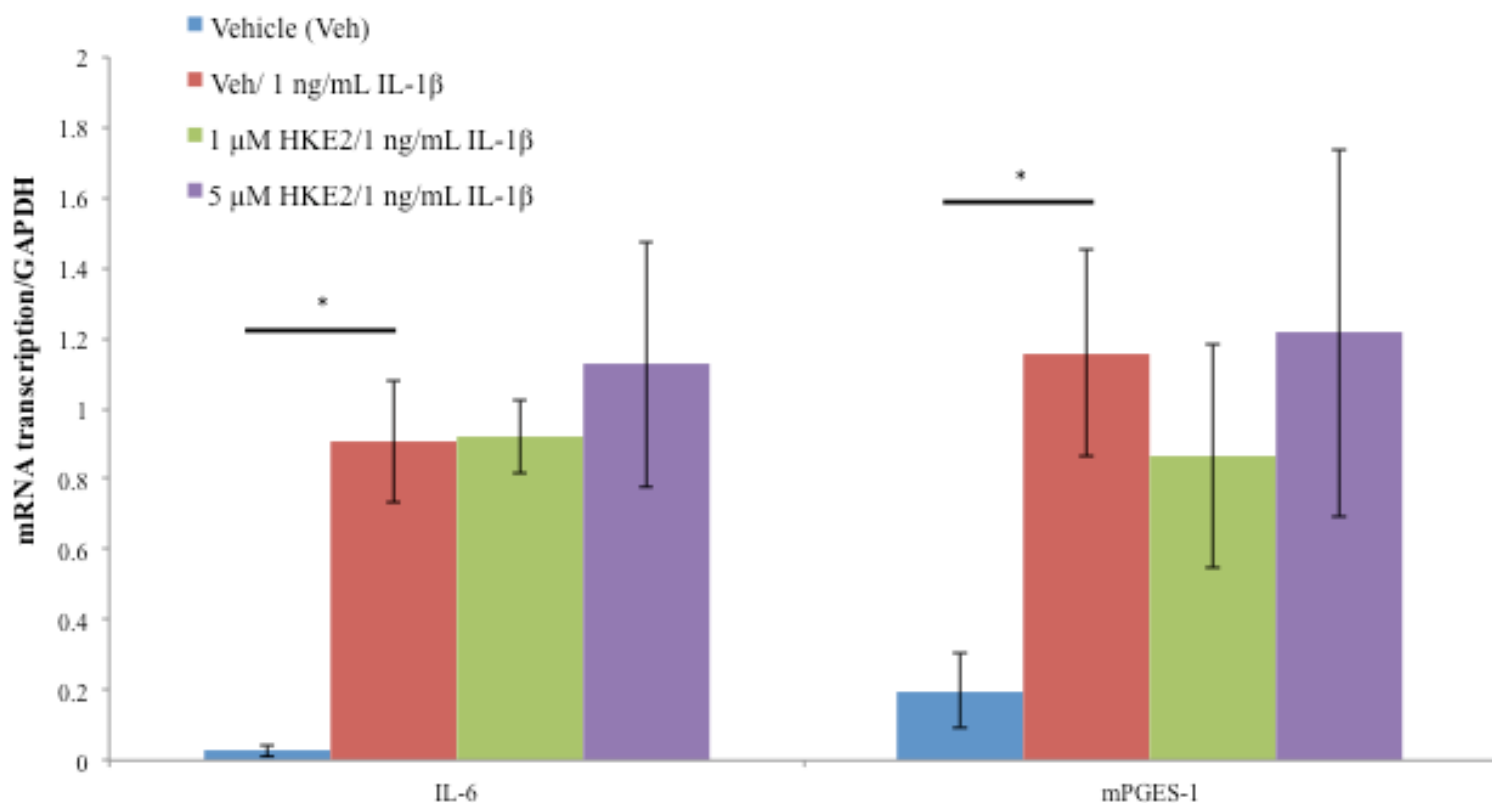


Figure 5: RT-qPCR analysis of hemiketal E₂ (HKE₂) modulation of interleukin-1 β induced changes to IL-6 and mPGES-1 gene transcription in primary human synovial fibroblasts. Changes in gene transcription are shown relative to the reference gene GAPDH. Error bars represent standard error of the mean (* = $p < 0.01$, unpaired t test, $n = 3$).

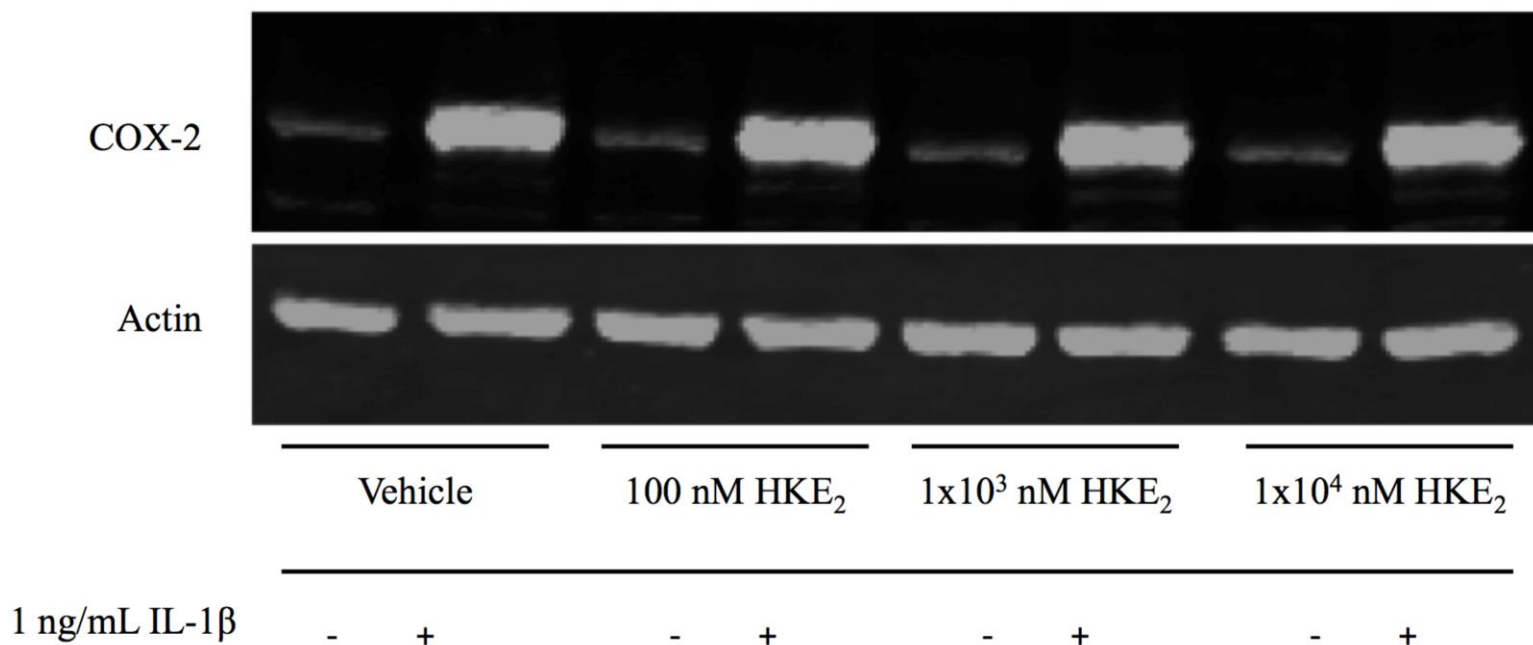


Figure 6: Western blot analysis of COX-2 expression as modulated by hemiketal eicosanoid E₂ (HKE₂) in human primary synovial fibroblasts. Primary synovial fibroblasts were treated with indicated concentrations of hemiketal E₂ for 45 min then stimulated with 1 ng/mL IL-1β for 6 h at which point protein lysates were collected and subjected to Western blot analysis. (n =3).

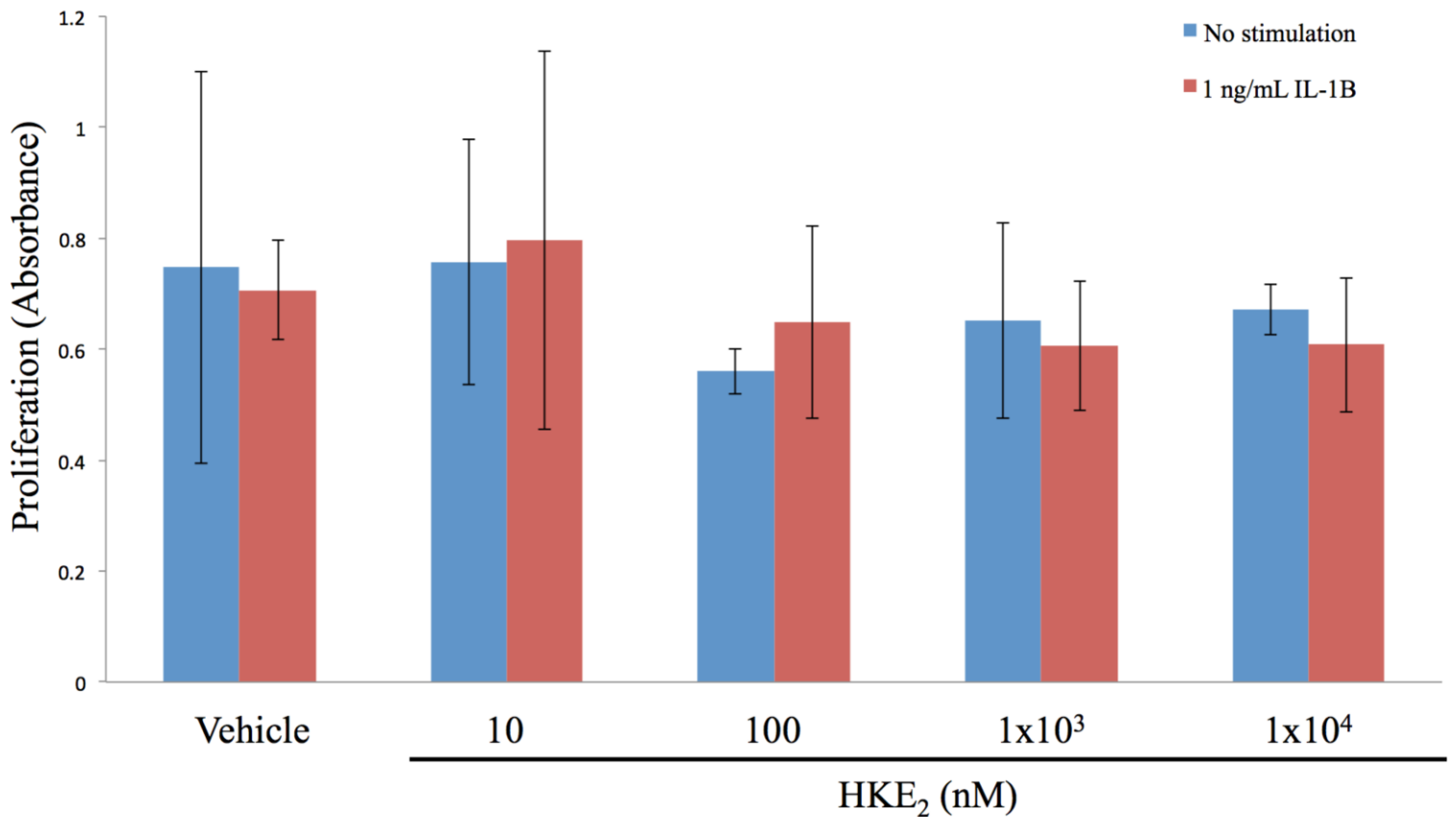


Figure 7: WST-1 cell proliferation assay to measure the effects of hemiketal eicosanoid E₂ (HKE₂) on proliferation of primary human synovial fibroblasts. Primary synovial fibroblasts were treated with increasing concentrations of HKE₂ in the presence and absence of interleukin 1 β to measure cell proliferation at 24 h in treated cells versus control (Vehicle-treated) cells. Error bars represent standard error of the mean (n = 3).

CHAPTER IV

Testing the Effects of Hemiketal E₂ in Human Umbilical Vein Endothelial Cells

Introduction

Since both COX-2 and 5-LOX products have been implicated in endothelial cell regulation, in 2011 the Schneider lab tested the effects of HKs on mouse microvascular pulmonary endothelial cells^{2,34}. The lab demonstrated that HKE₂ and HKD₂ potently stimulated tubulogenesis in mouse microvascular endothelial cells at nanomolar concentrations². For this reason, we hypothesized that HKE₂ would also stimulate tubulogenesis, a step in angiogenesis in HUVECs. The steps of angiogenesis are (1) vascular sprouting, (2) tubule morphogenesis, (3) adaptation to tissue needs, and (4) vessel stabilization. During tubulogenesis a cell must establish apicobasal polarity. Tubulogenesis involves complex cellular interaction with extracellular matrix, along with cytoskeletal reorganization, and the underlying mechanisms of this process still require elucidation^{35,36}. Several important variables in tubulogenesis are factors such as cell polarity^{35,37}, cytoskeletal factors, and matrix metalloproteinases.

Well-established angiogenesis assays use endothelial cells to measure cell proliferation, cell migration, and tube formation as a part of the overall process^{36,38,39}. While it is logical that HKs may exert an effect at any stage of angiogenesis, especially under inflammatory conditions such as wounding or cardiovascular disease, we chose to use tube formation as a measure of HK effect because of the positive results using mouse microvascular pulmonary endothelial cells, and in the event of a positive result it would be easier to focus in from the wider result of tube formation.

Results and discussion

To examine the effect of HKE₂ on tubulogenesis in HUVECs cell culture medium containing vehicle, various concentrations of HKE₂, or complete endothelial cell culture medium containing 5% fetal bovine serum (FBS) was added to cells. HUVECs were allowed to incubate for 6 h under serum starved conditions (except for the positive control wells), at which point medium was removed and cells were fixed in formalin. The number of tubes per visual field were counted and quantified (Figure 8). Representative images are shown in Figure 9. No visible difference between vehicle and HKE₂ treated cells were seen, while cells treated with complete medium visibly formed more tubes. While not included in the quantification, multiple repeats of higher concentration HKE₂ treatments were performed (1 μM and 10 μM). HKE₂ appeared to have no effect at the higher concentrations. HKE₂ does not stimulate (or inhibit) tubulogenesis of primary HUVECs compared to no treatment.

We also examined the effect of HKE₂ on proliferation of HUVECs after 24 h exposure to concentrations of HKE₂ ranging from 10 nM to 10 μM. HKE₂ showed no effect on proliferation, neither stimulating nor inhibiting proliferation. We also examined if HKE₂ effected proliferation in HUVECs that we stimulated with 1 ng/mL IL-1β. Again, HKE₂ demonstrated no effect on proliferation in HUVECs (Figure 10).

Conclusions

While HKE₂ stimulated tubulogenesis in primary mouse microvascular endothelial cells, we were unable to replicate this result in HUVECs. We also did not see that HKE₂ effected proliferation of HUVECs over a broad range of concentrations after 24 h. As in the primary

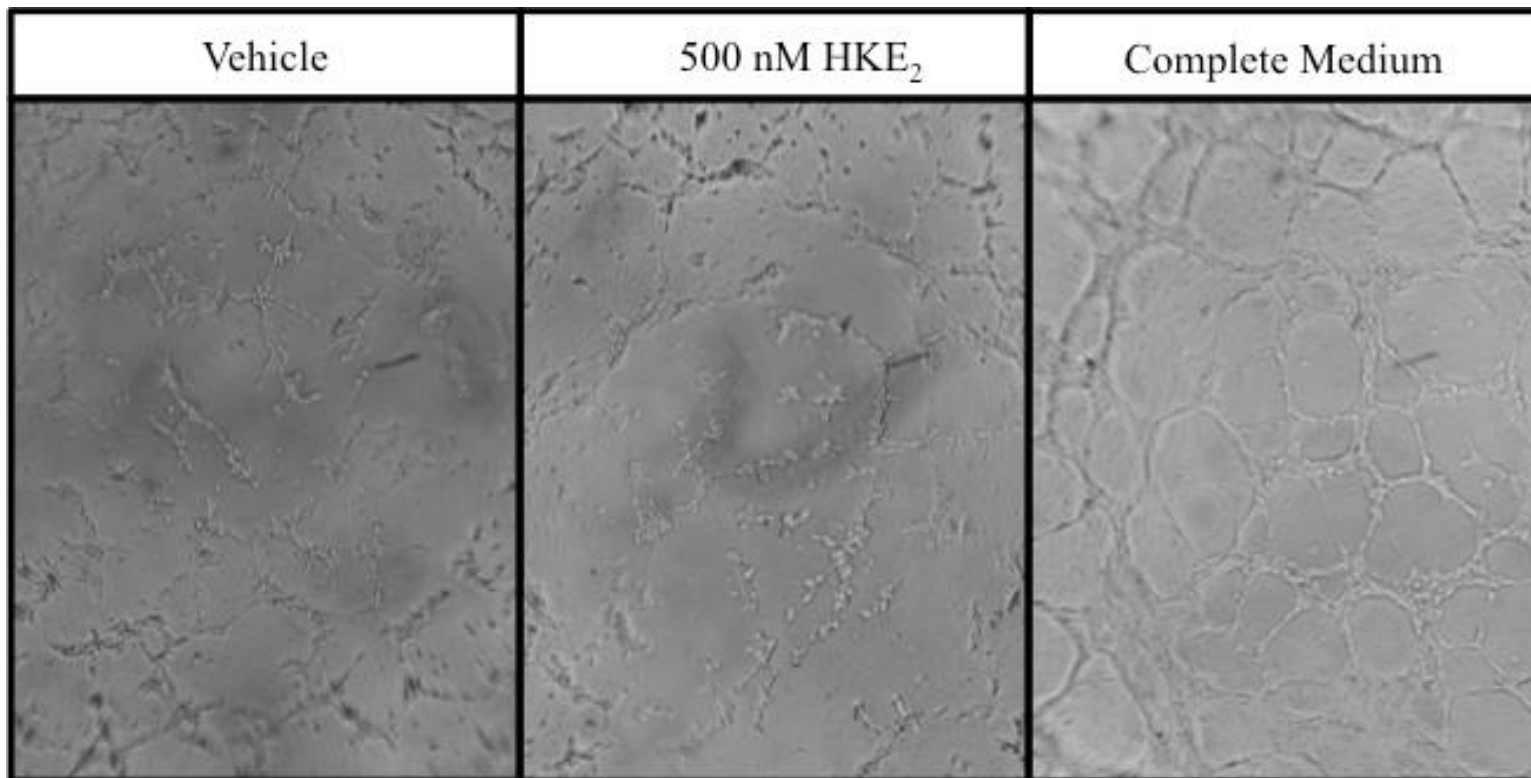


Figure 8: Hemiketal E₂ (HKE₂) effects on tubulogenesis in human umbilical vein endothelial cells (HUVECs). HUVECs were seeded at 2.5×10^3 cells per wells onto matrigel and allowed to grow in the presence and absence of no treatment, vehicle, HKE₂, and complete endothelial cell medium containing 10% FBS (n = 3).

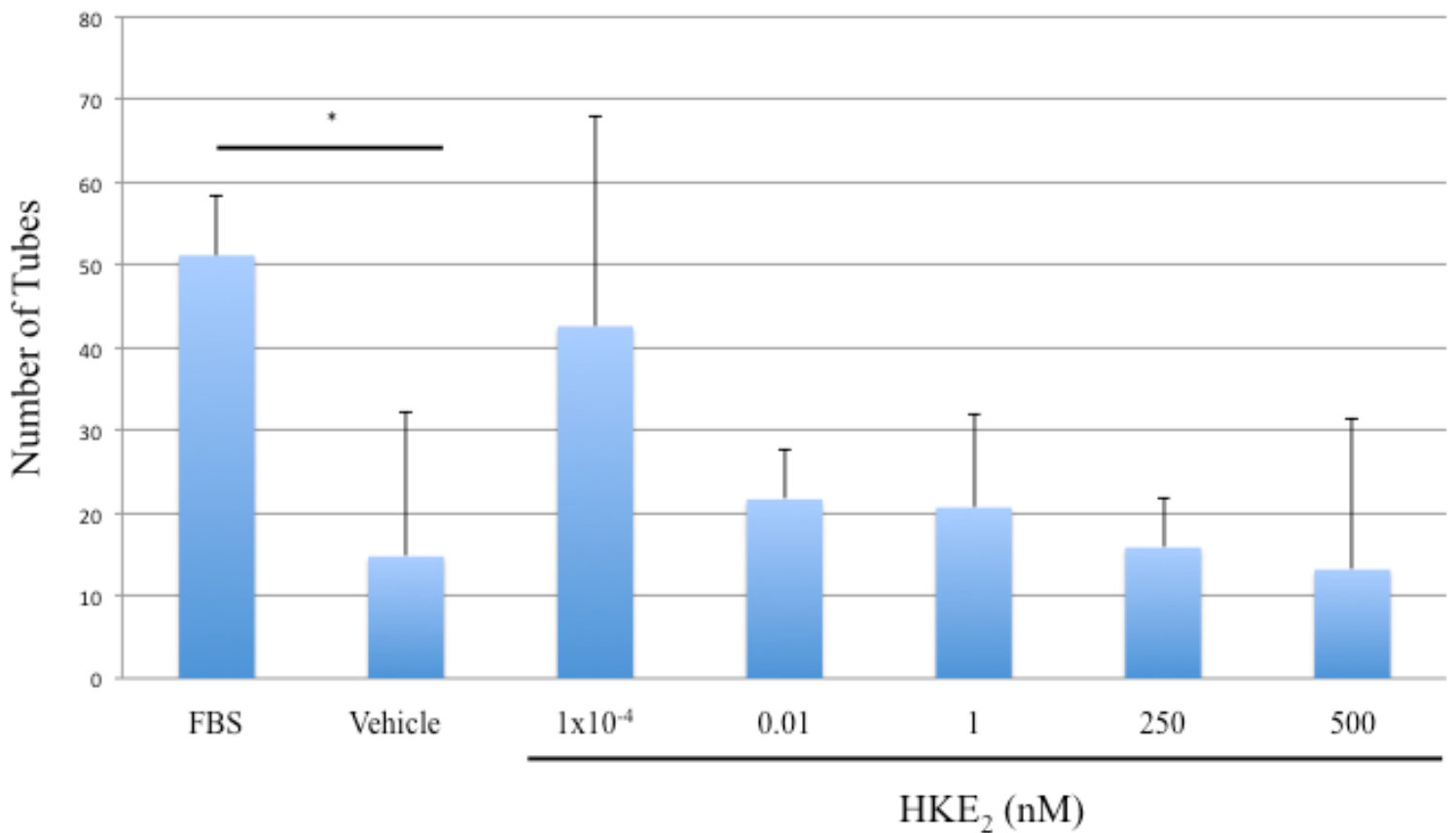


Figure 9: Quantification of hemiketal E₂ (HKE₂) effects on tubulogenesis in human umbilical vein endothelial cells (HUVECs). HUVECs were seeded at 2.5×10^3 cells per wells onto matrigel and allowed to grow in the presence and absence of no treatment, vehicle, HKE₂, and complete endothelial cell medium containing 10% FBS. After 6 h the cells were fixed with formalin. Each well was imaged using light microscopy, and the number of fully closed tubelike structures was tallied for each condition. Error bars represent standard error of the mean (* = $p < 0.02$, unpaired t test, $n=3$).

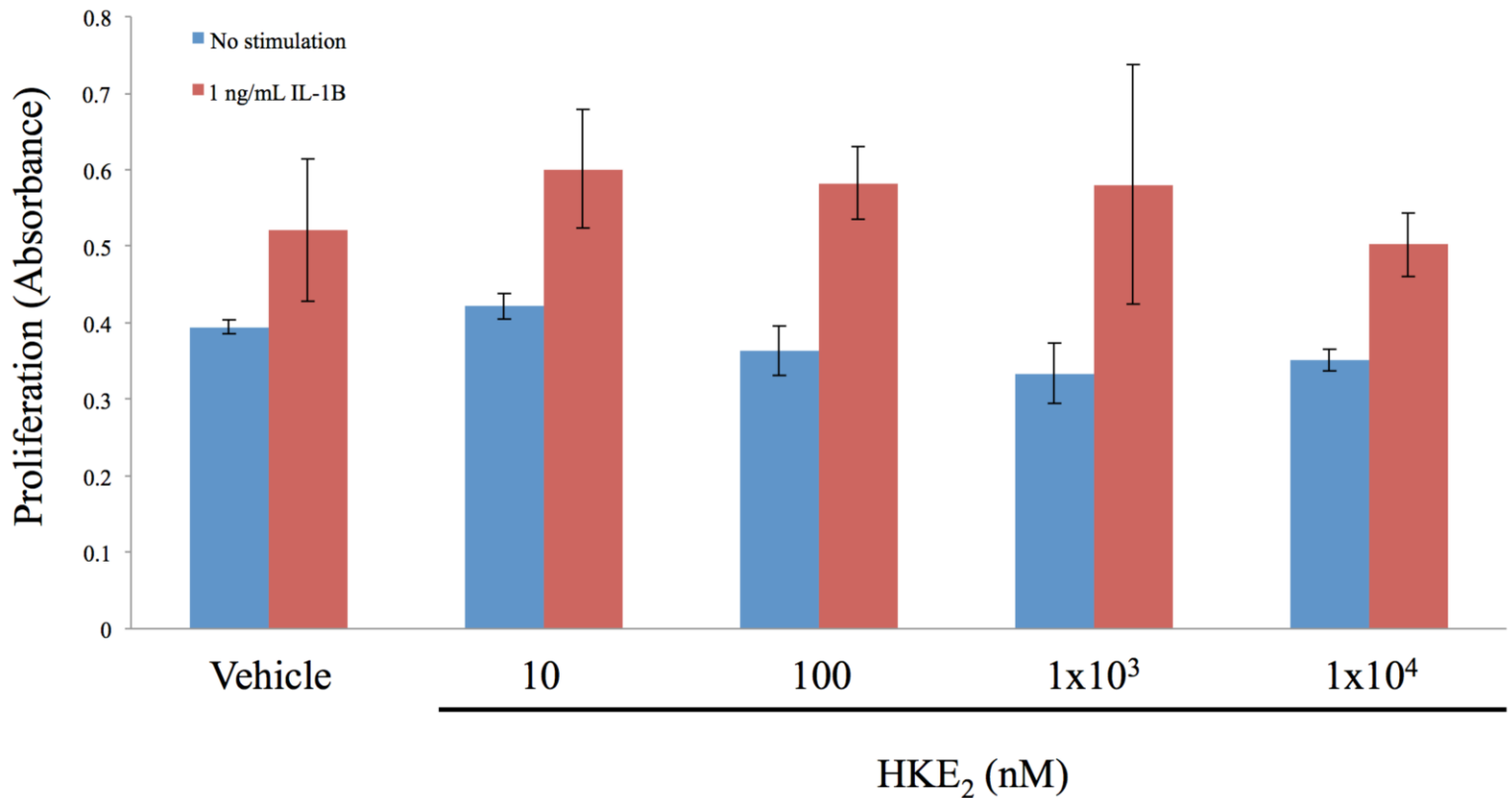


Figure 10: WST-1 cell proliferation assay to measure the effects of hemiketal eicosanoid E₂ (HKE₂) on proliferation of human umbilical vein endothelial cells (HUVECs). HUVECs were treated with increasing concentrations of HKE₂ in the presence and absence of interleukin 1 β to measure cell proliferation at 24 h in treated cells versus control (vehicle-treated) cells. Error bars represent standard error of the mean (n=3).

synovial fibroblasts, it would be remiss to conclude that HKE₂ does not produce a biological response in HUVECs. The conclusion is simply that in the models tested HKE₂ does not produce the biological response that we were measuring. Initial data (not shown) suggests that 500 nM HKE₂ may stimulate ERK1/2 phosphorylation, as well as P38 phosphorylation. This means that there is a possible biological effect of HKE₂, but that the circumstances under which HKE₂ acts is more complex than the system we modeled.

CHAPTER V

Testing the Effects of Hemiketal E₂ in RAW 264.7 Cells

Introduction

The RAW 264.7 cell line is a cell line derived from murine tumors that were induced with Abelson leukemia virus. This cell line exhibits many properties of macrophages, for example it can take up neutral red dye, can synthesize and secrete lysozyme, can phagocytose latex and zymosan beads⁴⁰, and can be induced to robustly express COX-2. Griesser, et al. have shown that RAW 264.7 cells are able to synthesize HKs when the 5-LOX product 5S-HETE is added exogenously and that human leukocyte samples (containing COX-2 expressing macrophages and 5-LOX expressing neutrophils) can be stimulated to produce HKs². For these reasons we conjectured that RAW 264.7 cells would be a suitable model for testing the biological effects of HKE₂.

Since eicosanoids modulate NFκB signaling in RAW 264.7 cells⁴¹, we used RAW 264.7 cells with a stable transfection of pNFκB-MetLuc2 (reporter vector) to monitor NFκB activation. This vector has NFκB binding consensus enhancer sequences cloned in the promoter region, such that when NFκB is activated and translocates to the nucleus, the activated complex will bind to the cloned region and initiate the transcription of the secreted *Metridia* luciferase reporter gene. COX-2 expression is highly inducible in RAW 264.7 cells, and has shown to be regulated by eicosanoids. It has also been demonstrated that PGE₂, a COX-2 product to which HKE₂ bears structural similarity, mediates suppression of phagocytosis in macrophages⁴². Due to the established connection of macrophage regulation by eicosanoids, the proximity of COX-2

expressing macrophages to 5-LOX expressing neutrophils, we believed RAW 264.7 cells to be a relevant model in which to examine HKE₂ activity.

Results and discussion

To examine the effect of HKE₂ on COX-2 expression in RAW 264.7 cells, cells were treated with various concentration of HKE₂ (as indicated) after 45 min 100 ng/mL LPS was added (or not). HKE₂ did not effect COX-2 expression in stimulated or unstimulated RAW 264.7 cells (Figure 11). Similarly, enzyme-linked immunosorbent assays (ELISAs) were carried out using RAW 264.7 cells, and the same treatment conditions as mentioned previously, but the supernatant was collected to measure levels of PGE₂. PGE₂ levels, relatively, reflect COX-2 expression based on treatments (Figure 12).

We also examined the ability of HKE₂ to modulate NFκB activation in pNFκB-MetLuc2 stably transfected RAW 264.7 cells. Cells were treated with the indicated concentrations of HKE₂ for 45 min. After 45 min cells were stimulated with 1 ng/mL LPS to activate NFκB. This cell line expresses NFκB binding consensus enhancer sequences cloned in the promoter region. When NFκB is activated and translocates to the nucleus, the activated complex will bind to the cloned region and will initiate the transcription of the secreted *Metridia* luciferase reporter gene. Luciferase activity is measured in the supernatant (Figure 13). Our results show that HKE₂ has no effect on NFκB activation. We also found that HKE₂ independent of LPS has no effect on the activation of NFκB (data not shown).

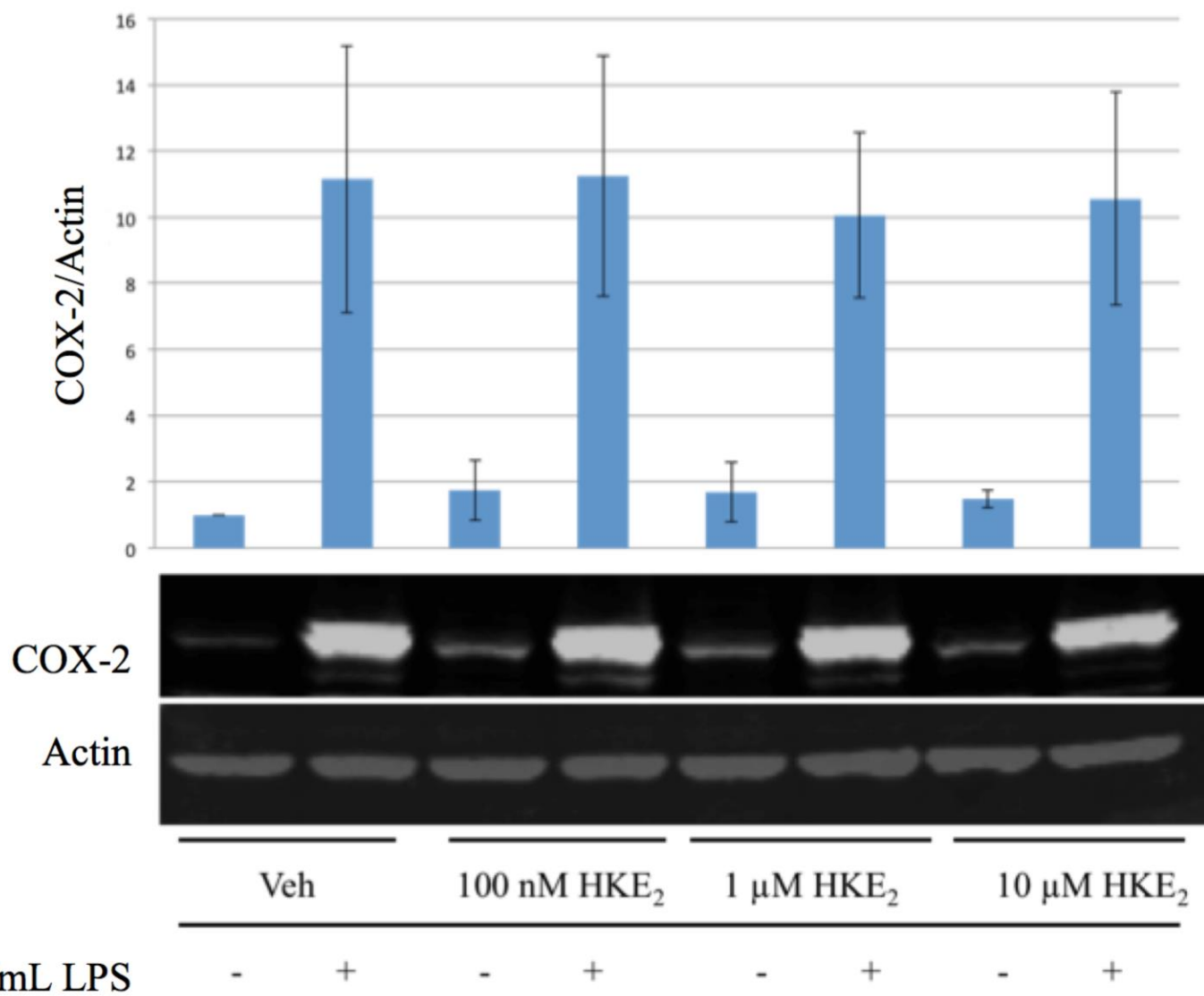


Figure 11: Western blot analysis of COX-2 expression as modulated by hemiketal eicosanoid E₂ (HKE₂) in RAW 264.7 cells. RAW 264.7 cells were treated with indicated concentrations of hemiketal E₂ for 45 min then stimulated with lipopolysaccharide from *E. coli* 0111:B4 for 6 h at which point protein lysates were collected and subjected to Western blot analysis. The quantification of the Western blot analyses is shown above. Error bars represent standard error of the mean (n=3).

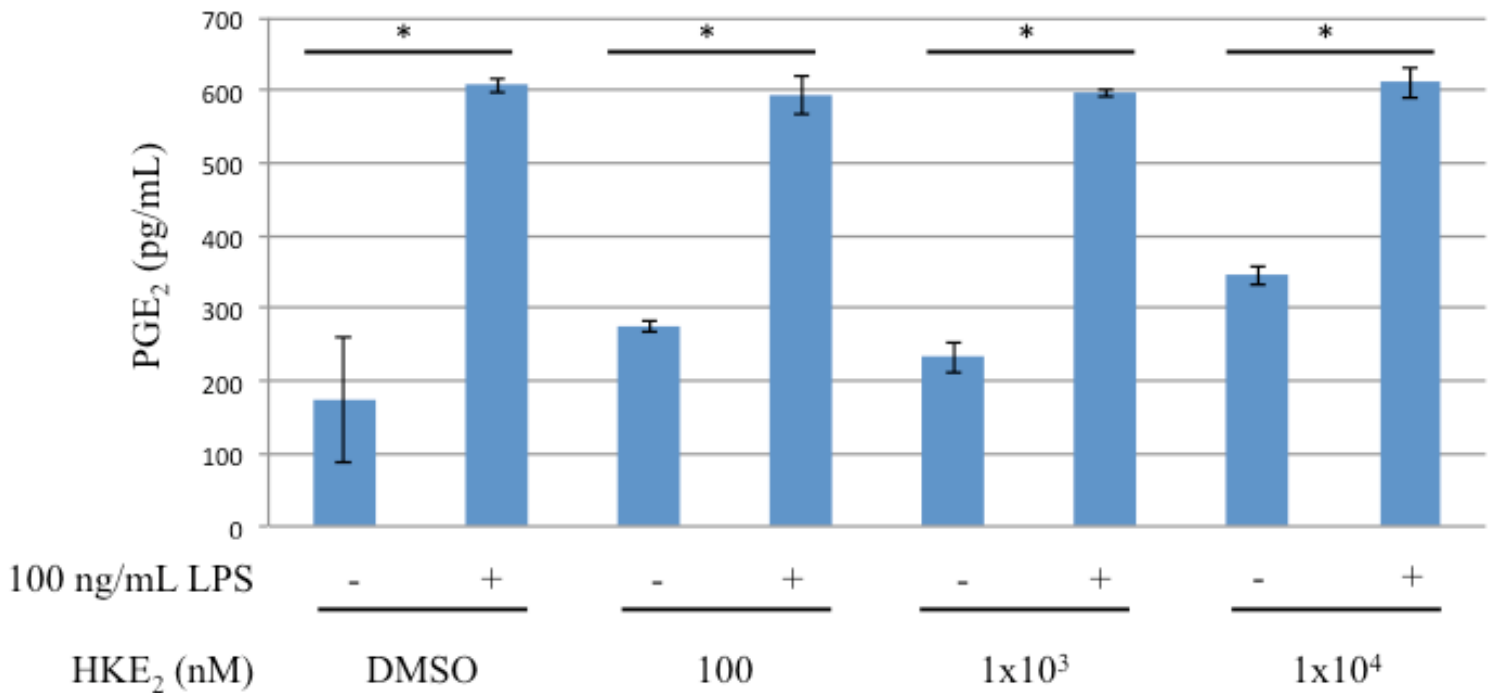


Figure 12: ELISA analysis of PGE₂ levels as modulated by hemiketal eicosanoid E₂ (HKE₂) in RAW 264.7 cells. RAW 264.7 cells were treated with indicated concentrations of hemiketal E₂ for 45 min then stimulated with lipopolysaccharide from *E. coli* 0111:B4 for 6 h at which point culture medium was collected and subjected to ELISA. Error bars represent standard error of the mean (* = p < 0.01, unpaired t test, n=2).

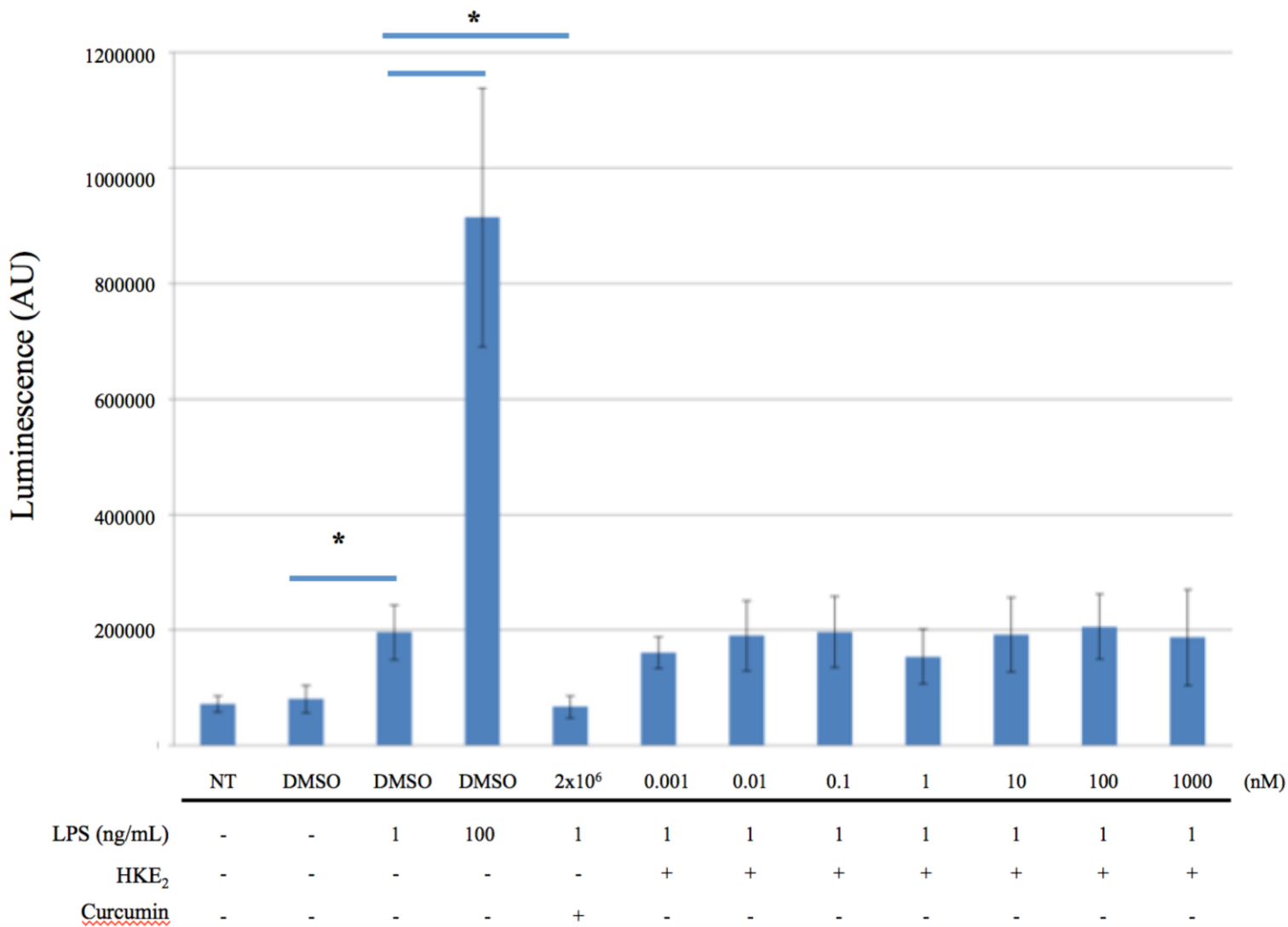


Figure 13: Effect of hemiketal eicosanoid E₂ (HKE₂) effect on NFκB activation in pNFκB-MetLuc2 stably transfected RAW 264.7 cells. To interrogate activation of NFκB by HKE₂ was preincubated with pNFκB-MetLuc2 stably transfected RAW 264.7 cells at the above described concentrations. Cells were then stimulated with 1 ng/mL lipopolysaccharide from *E. coli* 0111:B4. Error bars represent standard error of the mean (p<0.01, unpaired t test, n=3).

To examine the effect of HKE₂ on proliferation of RAW 264.7 cells after 24 h exposure to concentrations of HKE₂ ranging from 10 nM to 10 μM. HKE₂ showed no effect on proliferation, neither stimulating nor inhibiting proliferation. We also measured proliferation in RAW 264.7 cells that we stimulated with 100 ng/mL LPS. Again, HKE₂ demonstrated no effect on proliferation in RAW 264.7 cells (Figure 14).

We also measured the effect of HKE₂ on phagocytosis of fluorescently labeled *E. coli* particles. We selected a model system designed to quantitate how HKE₂ might effect phagocytic function of RAW 264.7 cells. The system used was selected to follow the internalization of a foreign, fluorescently labeled *E. coli* particles. We detected intracellular fluorescence emitted by the engulfed particles, as well as the effective fluorescence quenching of the extracellular probe (i.e. the particles not engulfed). RAW 264.7 cells were incubated with HKE₂ for 1 h, after which fluorescently tagged *E.coli* particles were added to the cells, thus stimulating phagocytosis. We found that HKE₂ does not appear to effect phagocytosis in RAW 264.7 cells (Figure 15). I will note this assay is worth repeating, as these trials were part of preliminary searches for possible HKE₂ activity. While we saw no apparent effect of HKE₂, the appropriate negative control of 10 μM Cytochalasin D incubation (to prevent phagocytosis) is missing from the assay.

Conclusions

HKE₂ does not appear to modulate NFκB, COX-2 expression, or PGE₂ levels in RAW 264.7 cells when exogenously administered and preincubated with this cell line 45 min prior to the addition of LPS. However, there are non-canonical pathways leading to the activation of NFκB and upregulation of COX-2⁴³. It is possible that HKE₂ might effect these inflammatory markers through a non-canonical mechanism. While we posit the HKE₂ plays a role in inflammation,

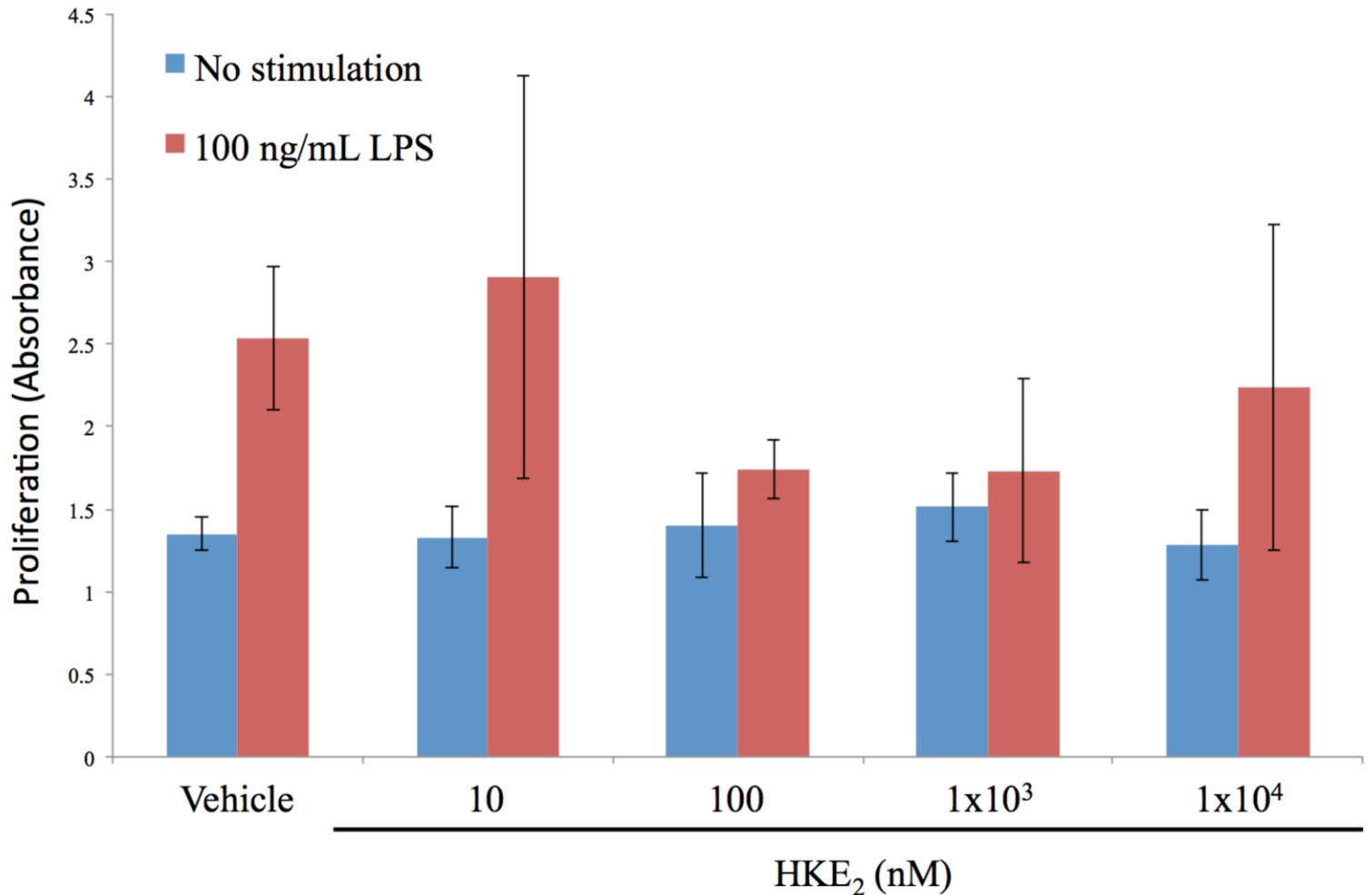


Figure 14: WST-1 cell proliferation assay to measure the effects of hemiketal eicosanoid E₂ (HKE₂) on proliferation of RAW 264.7 cells. RAW 264.7 cells were treated with increasing concentrations of HKE₂ in the presence and absence of 100 ng/mL lipopolysaccharide from *E. coli* 0111:B4 to measure cell proliferation at 24 h in treated cells versus control (Vehicle-treated) cells. Error bars represent standard error of the mean (n=3).

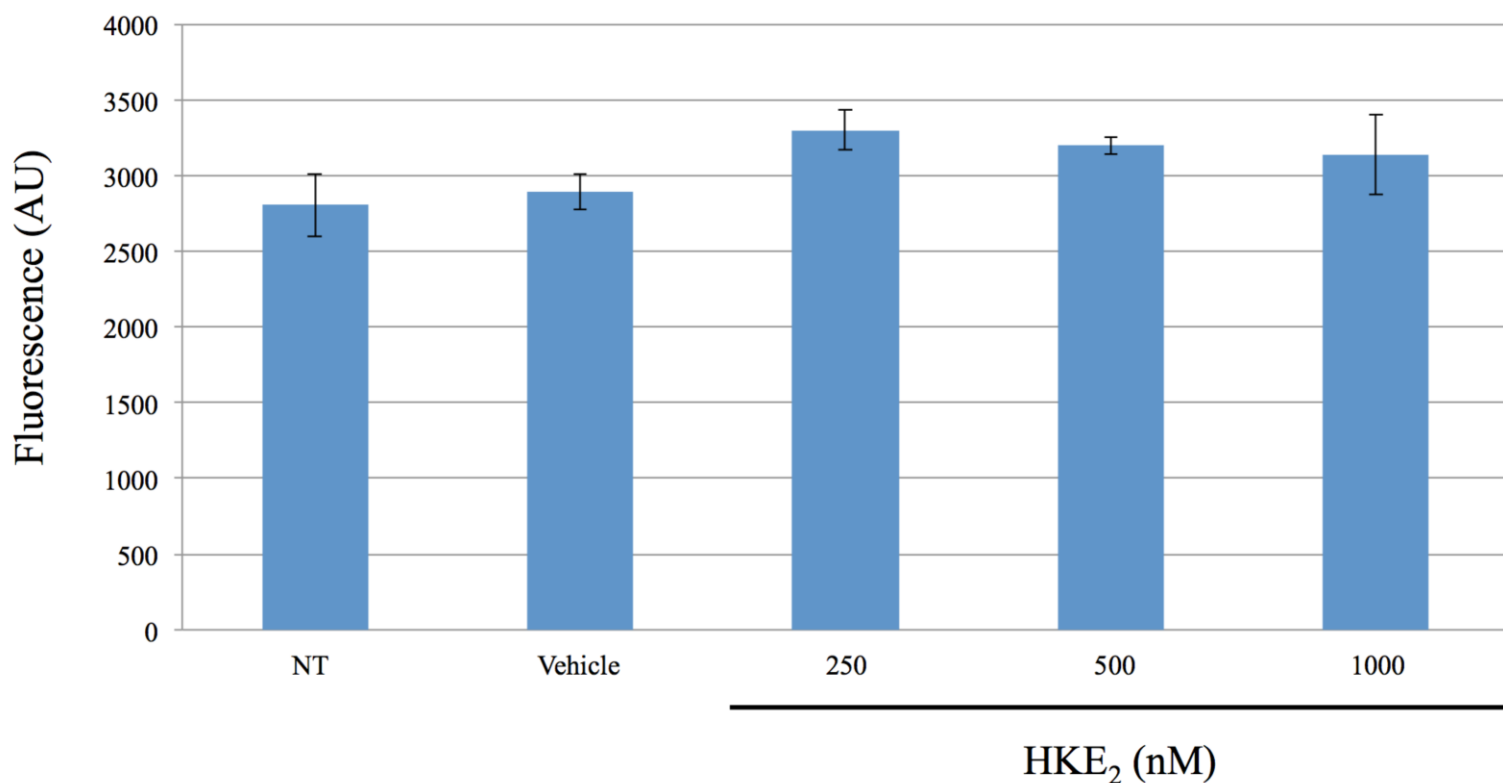


Figure 15: Fluorescent assay to measure the effects of hemiketal eicosanoid E₂ (HKE₂) on phagocytosis of fluorescently labeled *E. coli* particles. RAW 264.7 cells were treated with increasing concentrations of HKE₂ for 1 h, at which point the fluorescently labeled *E. coli* particles were added. To measure the effect of HKE₂ on phagocytosis by RAW 264.7 fluorescence was monitored. Error bars represent standard error of the mean (n=2).

understanding the role of HKE₂ in non-canonical signaling may be worth investigating further.

HKE₂ also does not appear to effect proliferation of RAW 264.7 cells or the ability of RAW

264.7 cells to phagocytose fluorescently tagged *E. coli* particles.

CHAPTER VI

Materials and Methods

Cell lines, cell culture and reagents

Primary synovial fibroblasts were a gift of Dr. Leslie Crofford (Professor of Pathology, Microbiology, and Immunology, Vanderbilt University Medical Center). Primary, pooled donor HUVECs were purchased from Lonza (USA). RAW 264.7 cells were obtained from ATCC (Manassas, VA). Primary synovial fibroblasts were maintained in Dulbecco's Modified Eagle Medium (Invitrogen, Carlsbad, CA) supplemented with 20% fetal bovine serum (Gemini Bio Products, West Sacramento, CA), 100 U/mL penicillin, and 100 µg/ mL streptomycin (Invitrogen). HUVECs were maintained in EGM-2 medium, supplemented with human Epidermal Growth Factor, Vascular Endothelial Growth Factor, R3-Insulin-like Growth Factor-1, Ascorbic Acid, Hydrocortisone, human Fibroblast Growth Factor-Beta, Heparin, Fetal Bovine Serum, and Gentamicin/Amphotericin-B. RAW 264.7 cells were maintained in Dulbecco's Modified Eagle Medium (Invitrogen, Carlsbad, CA) supplemented with 10% fetal bovine serum (Gemini Bio Products, West Sacramento, CA), 100 U/mL penicillin, and 100 µg/ mL streptomycin (Invitrogen). All cells were maintained at 37 °C in an atmosphere of 5% CO₂ at a confluence of 80% or less.

HPLC, LC-MS/MS and analytical reagents

HKE₂ was analyzed and purified by UV/Vis-HPLC using a Waters Symmetry C18 column (4.6 x 250 mm; 5 µm) eluted with a gradient of 20% acetonitrile (Sigma) to 70%

acetonitrile in 0.01% aqueous acetic acid over 25 min. Elution of the products was monitored using an Agilent 1200 diode array detector.

A TSQ Vantage Triple Stage Quadrupole LC/MS Mass Spectrometer (Thermo Scientific) with an electrospray interface was linked to an Agilent 1100 series HPLC and operated in the negative ion mode. Settings for sheath and auxiliary gas pressures, temperature, and interface voltage were optimized based on previous experiments². A Waters Symmetry Shield C18 3.5 μm column (2.1 x 150 mm) was used with a linear gradient of acetonitrile/water, 10 mM NH_4OAc (5/95; solvent A) to acetonitrile/water, 10 mM NH_4OAc (95/5 by volume solvent B) at 0.5 mL/min within 5 min. For HKE2 the transition m/z 399 \rightarrow 151 was monitored in the negative ion SRM mode.

Tubulogenesis assay

For the Matrigel-based tubulogenesis assay capillary-like structure formation of HUVECs was analyzed as number of closed tube-like structures formed³⁸. Cooled 96-well plates were coated with 50 μL of BD Matrigel Matrix Growth Factor Reduced (BD Biosciences) and incubated for 30 min at 37 $^\circ\text{C}$. Wells were fixed in formalin after 6 h and number of tube-like structures was quantified using images from a Nikon Eclipse 50i microscope using a 10x objective. Images were processed using ACT-1C Software.

WST-1 cell proliferation assay

The effects of HKE₂ on proliferation in primary synovial fibroblasts, HUVECs, and RAW 264.7 cells were examined using the WST-1 assay. Per manufacturer's instruction 100 μL per well of cells (5.0×10^3 cells per well for primary synovial fibroblasts, 2.5×10^4 cells per well

for HUVECs, and 4.0×10^4 for RAW 264.7 cells) were added in a 96-well plate, and incubated in serum free medium for 24 h in the presence or absence of varying concentrations of HKE₂ (as indicated), with or without inflammatory stimulus (1 ng/mL IL-1 β for synovial fibroblasts or 100 ng/mL LPS for RAW 264.7 cells). After 24 h, 10 μ L of WST-1 reagent was added to each well, and cells were incubated for another 4 hours, per manufacturer's instructions. The absorbance of the samples was then measured at 490nm with a microplate reader (Molecular Device, California) after shaking for 1 min against the blank, a background control. Each assay was run with technical triplicates, and was repeated 3 separate times. Cell proliferation assays were in triplicates.

Western blot analysis

For measuring COX-2 expression cells were plated on 10-cm cell culture dishes and allowed to grow for 48 h. The cell culture medium was removed, cells were washed, and serum free medium containing various concentration of HKE₂ was added. After 45 min, 1 ng/mL IL-1 β for synovial fibroblasts or 100 ng/mL LPS for RAW 264.7 cells was added. Cells were allowed to incubate for 6 hours, at which point the medium was removed, cells were washed and then scraped from the cell culture plate into 6 mL cold PBS using a cell lifter (Corning Incorporated, Corning, NY). Cells were then centrifuged at 1000 xg for 5 minutes. The PBS supernatant was aspirated and the cell pellet was resuspended in cold PBS followed by centrifugation at 5000 RPM for 5 minutes to wash the cells. Cell lysates were prepared by aspirating the PBS supernatant and lysing the cells in an appropriate volume of RIPA buffer containing protease inhibitors (Roche) and phosphatase inhibitors (Roche). Protein concentration of cell lysates was determined using the bicinchoninic acid (BCA) assay (Pierce, Rockford, IL) according to the

manufacturer's instructions. Cell lysate samples were then diluted into NuPAGE LDS Sample Buffer (4X) (Novex, Carlsbad, CA) and boiled at 95 °C for 10 minutes. Cell lysate samples were loaded on 10% SDS-PAGE gel and resolved via electrophoresis at 100 V for approximately 1.5 hours in sodium dodecyl sulfate (SDS) buffer (Novex). After gel electrophoresis samples were transferred overnight onto nitrocellulose membranes (Whatman, Little Chalfont, UK) by electrophoresis at 10 V in SDS/Glycine Buffer (Bio-Rad, Hercules, CA) with 20% methanol (Sigma-Aldrich). The membranes were probed with the mouse monoclonal anti-COX-2 (aa 684-598) (1:1000 dilution; Cayman Chemical, Ann Arbor, MI) and mouse monoclonal anti-GAPDH (1:2000 dilution; Abcam, Cambridge, UK). Following primary antibody incubation, membranes were incubated with horseradish peroxidase (HRP)-conjugated polyclonal anti-mouse or anti-rabbit immunoglobulin (IgG) (1:10,000 Promega, Madison, WI) and then visualized using ECL Prime Western Blotting Detection Reagent (Amersham, Buckinghamshire, UK).

PGE₂ ELISA

RAW 264.7 cells were stimulated and treated with HKE₂ for 45 min then stimulated with 100 ng/mL LPS for 6 h. Supernatant was removed, spun at 1000 x g for 10 min at 4 °C for 10 min to pellet debris. The amount of PGE₂ in the supernatant was determined using PGE₂ ELISA Kit – Monoclonal (Cayman Chemical).

NFκB reporter assay

The RAW 264.7 cells were stable transfected by Rebecca Edwards in the Claus Schneider group with a pNFκB-MetLuc2 (reporter vector) to monitor NFκB activation. This pNFκB-MetLuc2 vector has NFκB binding consensus enhancer sequences cloned in the promoter region.

This means that when NFkB is activated and translocates to the nucleus, the activated complex binds the cloned region and initiates the transcription of the secreted *Metridia* luciferase reporter gene (Clontech Laboratories Inc., California).

REFERENCES

1. Schneider, C., Boeglin, W. E., Yin, H., Stec, D. F. & Voehler, M. Convergent Oxygenation of Arachidonic Acid by 5-Lipoxygenase and. 720–721 (2006).
2. Griesser, M. *et al.* Biosynthesis of hemiketal eicosanoids by cross-over of the 5-lipoxygenase and cyclooxygenase-2 pathways. *Proc. Natl. Acad. Sci. U. S. A.* **108**, 6945–50 (2011).
3. Funk, C. D. Prostaglandins and leukotrienes: advances in eicosanoid biology. *Science* **294**, 1871–5 (2001).
4. Simmons, D. L., Botting, R. M. & Hla, T. Cyclooxygenase Isozymes : The Biology of Prostaglandin Synthesis and Inhibition. **56**, 387–437 (2004).
5. Charlier, C. & Michaux, C. Dual inhibition of cyclooxygenase-2 (COX-2) and 5-lipoxygenase (5-LOX) as a new strategy to provide safer non-steroidal anti-inflammatory drugs. *Eur. J. Med. Chem.* **38**, 645–659 (2003).
6. Peters-Golden, M. & Henderson Jr., W. R. Leukotrienes. *N. Engl. J. Med.* **357**, 1841–1854 (2007).
7. Poeckel, D. & Funk, C. D. The 5-lipoxygenase/leukotriene pathway in preclinical models of cardiovascular disease. *Cardiovasc. Res.* **86**, 243–53 (2010).
8. Söderström, M., Wigren, J., Surapureddi, S., Glass, C. K. & Hammarström, S. Novel prostaglandin D₂-derived activators of peroxisome proliferator-activated receptor- γ are formed in macrophage cell cultures. *Biochim. Biophys. Acta - Mol. Cell Biol. Lipids* **1631**, 35–41 (2003).
9. Narala, V. R. *et al.* Leukotriene B₄ is a physiologically relevant endogenous peroxisome

- proliferator-activated receptor-alpha agonist. *J. Biol. Chem.* **285**, 22067–74 (2010).
10. Rådmark, O., Werz, O., Steinhilber, D. & Samuelsson, B. 5-Lipoxygenase: regulation of expression and enzyme activity. *Trends Biochem. Sci.* **32**, 332–41 (2007).
 11. Fürstenberger, G., Krieg, P., Müller-Decker, K. & Habenicht, a J. R. What are cyclooxygenases and lipoxygenases doing in the driver's seat of carcinogenesis? *Int. J. Cancer* **119**, 2247–54 (2006).
 12. Wang, X. *et al.* Co-expression of COX-2 and 5-LO in primary glioblastoma is associated with poor prognosis. *J. Neurooncol.* **125**, 277–285 (2015).
 13. Serhan, C. N. *et al.* Resolution of inflammation: state of the art, definitions and terms. *FASEB J.* **21**, 325–332 (2007).
 14. Serhan, C. N. & Savill, J. Resolution of inflammation: the beginning programs the end. *Nat. Immunol.* **6**, 1191–1197 (2005).
 15. Soehnlein, O. & Lindbom, L. Phagocyte partnership during the onset and resolution of inflammation. *Nat. Rev. Immunol.* **10**, 427–439 (2010).
 16. Gilroy, D. W. & Colville-Nash, P. R. New insights into the role of COX 2 in inflammation. *J. Mol. Med.* **78**, 121–129 (2000).
 17. Li, a C. *et al.* Peroxisome proliferator-activated receptor gamma ligands inhibit development of atherosclerosis in LDL receptor-deficient mice. *J. Clin. Invest.* **106**, 523–31 (2000).
 18. Gilroy, D. W., Lawrence, T., Perretti, M. & Rossi, A. G. Inflammatory resolution: new opportunities for drug discovery. *Nat. Rev. Drug Discov.* **3**, 401–16 (2004).
 19. McMahon, B. & Godson, C. Lipoxins: endogenous regulators of inflammation. *Am. J. Physiol. Renal Physiol.* **286**, F189–201 (2004).

20. Lowin, T. & Straub, R. H. Synovial fibroblasts integrate inflammatory and neuroendocrine stimuli to drive rheumatoid arthritis. *Expert Rev. Clin. Immunol.* 1–3 (2015). doi:10.1586/1744666X.2015.1066674
21. Sano, H. *et al.* In vivo cyclooxygenase expression in synovial tissues of patients with rheumatoid arthritis and osteoarthritis and rats with adjuvant and streptococcal cell wall arthritis. *J. Clin. Invest.* **89**, 97–108 (1992).
22. Kolaczowska, E. & Kubes, P. Neutrophil recruitment and function in health and inflammation. *Nat. Rev. Immunol.* **13**, 159–75 (2013).
23. Rao, R. M., Yang, L., Garcia-Cardena, G. & Luscinskas, F. W. Endothelial-dependent mechanisms of leukocyte recruitment to the vascular wall. *Circ. Res.* **101**, 234–47 (2007).
24. Lefkowitz, D. L. & Lefkowitz, S. S. Macrophage-neutrophil interaction: a paradigm for chronic inflammation revisited. *Immunol. Cell Biol.* **79**, 502–6 (2001).
25. Snyder, N. W., Revello, S. D., Liu, X., Zhang, S. & Blair, I. a. Cellular uptake and antiproliferative effects of 11-oxo-eicosatetraenoic acid. *J. Lipid Res.* **54**, 3070–7 (2013).
26. Bligh, E.G. and Dyer, W. J. A Rapid Method of Total Lipid Extraction and Purification. *Can. J. Biochem. Physiol.* **37**, (1959).
27. Leclerc, P. *et al.* IL-1 β /HMGB1 Complexes Promote The PGE2 Biosynthesis Pathway in Synovial Fibroblasts. *Scand. J. Immunol.* **77**, 350–360 (2013).
28. Yuhki, K. *et al.* Roles of prostanoids in the pathogenesis of cardiovascular diseases: Novel insights from knockout mouse studies. *Pharmacol. Ther.* **129**, 195–205 (2011).
29. Crofford, L. J. COX-2 in synovial tissues. *Osteoarthr. Cartil.* **7**, 406–408 (1999).
30. Robinson, D. R., Tashjian, A. H. & Levine, L. Prostaglandin stimulated bone resorption by rheumatoid synovia. A possible mechanism for bone destruction in rheumatoid

- arthritis. *J. Clin. Invest.* **56**, 1181–1188 (1975).
31. Siegle, I. *et al.* Expression of cyclooxygenase 1 and cyclooxygenase 2 in human synovial tissue. *Arthritis Rheum.* **41**, 122–129 (1998).
 32. Hershko, D. D., Robb, B. W., Luo, G. & Hasselgren, P.-O. Multiple transcription factors regulating the IL-6 gene are activated by cAMP in cultured Caco-2 cells. *Am. J. Physiol. Regul. Integr. Comp. Physiol.* **283**, R1140–R1148 (2002).
 33. Li, F. & Zhu, Y. T. HGF-activated colonic fibroblasts mediates carcinogenesis of colonic epithelial cancer cells via PKC-cMET-ERK1/2-COX-2 signaling. *Cell. Signal.* **27**, 860–866 (2015).
 34. Lötzer, K. *et al.* 5-Lipoxygenase/cyclooxygenase-2 cross-talk through cysteinyl leukotriene receptor 2 in endothelial cells. *Prostaglandins Other Lipid Mediat.* **84**, 108–15 (2007).
 35. Iruela-Arispe, M. L. & Beitel, G. J. Tubulogenesis. *Development* **140**, 2851–2855 (2013).
 36. Tung, J. J., Tattersall, I. W. & Kitajewski, J. Tips, stalks, tubes: Notch-mediated cell fate determination and mechanisms of tubulogenesis during angiogenesis. *Cold Spring Harb. Perspect. Med.* **2**, (2012).
 37. Chung, S. *et al.* Serrano (sano) functions with the planar cell polarity genes to control tracheal tube length. *PLoS Genet.* **5**, (2009).
 38. Piqueras, L. *et al.* Activation of PPAR γ Induces Endothelial Cell Proliferation and Angiogenesis. *Arterioscler. Thromb. Vasc. Biol.* **27**, 63–69 (2007).
 39. Ribatti, D. & Crivellato, E. ‘Sprouting angiogenesis’, a reappraisal. *Dev. Biol.* **372**, 157–65 (2012).
 40. Raschke, W. C., Baird, S., Raplh, P. & Nakoinz, I. Functional Macrophage Cell Lines

- Transformed by Abelson Leukemia Virus. *Cell* **15**, 261–267 (1978).
41. Conte, E. *et al.* Nuclear factor-KB activation in human monocytes stimulated with lipopolysaccharide is inhibited by fibroblast conditioned medium and. *FEBS Lett.* **400**, 315–318 (1997).
 42. Medeiros, A. I., Serezani, C. H., Lee, S. P. & Peters-Golden, M. Efferocytosis impairs pulmonary macrophage and lung antibacterial function via PGE2/EP2 signaling. *J. Exp. Med.* **206**, 61–68 (2009).
 43. Andreakos, E. *et al.* Distinct pathways of LPS-induced NF- B activation and cytokine production in human myeloid and nonmyeloid cells defined by selective utilization of MyD88 and Mal / TIRAP. *Blood* **103**, 2229–2237 (2004).